Geophys. J. Int. (1993) **114**, 45–62

The inference of mantle viscosity from an inversion of the Fennoscandian relaxation spectrum

J. X. Mitrovica[1] and W. R. Peltier[2]

[1]*Harvard-Smithsonian, Center for Astrophysics, 60 Garden St, MS-42, Cambridge, MA 02138, USA*
[2]*Department of Physics, University of Toronto, Toronto, Ontario, M5S 1A7, Canada*

Accepted 1992 November 6. Received 1992 November 5; in original form 1992 March 30

SUMMARY

A formal inverse theory for mantle viscosity is here applied to a relaxation spectrum derived from the post-glacial uplift of Fennoscandia. The spectrum represents the set of eigenfrequencies (or inverse decay times) for the fundamental mode of viscous gravitational relaxation between the spherical harmonic degrees 14 to 45 and 65 to 80. Theoretical predictions of the eigenfrequencies are based upon the determination of the zeroes of the secular determinant function derived for a spherically symmetric, self-gravitating, visco-elastic planet. Differential kernels relating shifts in the eigenfrequencies to arbitrary perturbations in the radial viscosity profile (i.e. Fréchet kernels) are computed using the variational principle derived by Peltier (1976). The inversions are performed within the framework of non-linear Bayesian inference, and the problem has been parameterized in terms of the logarithm of viscosity.

The inversions have yielded a set of robust constraints which all models for the radial viscosity profile below Fennoscandia must satisfy. The *a posteriori* estimates and variance reduction are found to be insensitive to the *a priori* variance ascribed to the model layers. The constraints have, furthermore, been summarized into a set of *a posteriori* estimates of the average model viscosity value in radial regions consistent with the resolving power of the data (which decreases from a radial length scale of approximately 120 km at the base of the lithosphere to 1200 km at 1000 km depth; the data provide essentially no information regarding the mantle rheology below 1200 km depth). For example, for Earth models with a lithospheric thickness (LT) of 100 km, the volumetric average logarithm of viscosity in regions in the depth ranges 1040–400 km, 670–210 km and 235–100 km is constrained to be, respectively, 21.03 ± 0.09, 20.70 ± 0.08 and 20.37 ± 0.19. We have repeated the inversions for a number of assumed lithospheric thicknesses and have found that a relatively low-viscosity layer in the sublithospheric region (with respect to the underlying upper mantle) is required for LT $\leq$ 120 km. In this respect we have quantified the previously described trade-off between a decrease in the viscosity of this region and a decrease in LT (Cathles 1975).

In forward analyses of the glacial isostatic adjustment data set it is common to use Earth models with isoviscous upper and lower mantle regions. To investigate this 'two-layer' case we have also performed inversions which assume perfect correlation amongst the model layers in the upper and, separately, the lower mantle. Under this strict model space limitation, the inversions yield models with upper and lower mantle viscosities in the range 3.7×10^{20}–4.5×10^{20} Pa s and 2.2×10^{21}–1.9×10^{21} Pa s, respectively. (The ranges are obtained from a suite of inversions using lithospheric thickness from 70 km to 145 km.)

The *a posteriori* constraints generated from the Bayesian inversions are used together with a statistic based on the computed misfit to the Fennoscandian relaxation spectrum, to rule out a number of previously published viscosity models.

The constraints have also been used to construct a set of models which illustrate the non-uniqueness inherent to the *a posteriori* model space. We show, for example, that a model with a weak asthenosphere (down to 400 km depth) overlying an isoviscous 10^{21} Pa s deep mantle provides a good fit to the relaxation spectrum. This is also true of models with a thin sublithospheric low-viscosity zone overlying a two-layer deep mantle with a moderate (factor of about three) jump in viscosity across 670 km depth, and models (as described in the preceding paragraph) with a viscosity jump of between four and six across isoviscous upper and lower mantle regions. In a companion paper the *a posteriori* constraints derived herein are used as *a priori* constraints in the direct inversion of RSL observations from Fennoscandia in order to examine whether this imprecision in the inference is a manifestation of the non-uniqueness inherent to the totality of the Fennoscandian data.

Key words: Fennoscandia, inversion, mantle viscosity, relaxation spectrum.

1 INTRODUCTION

The inference of mantle viscosity from observations of the isostatic adjustment of the planet following the last major deglaciation event of the current ice age is a problem of continuing interest in geophysics. Historically (see Cathles 1975; Peltier 1982; Ekman 1991, for detailed reviews), the first quantitative estimates of mantle viscosity were based on the observed uplift of Fennoscandia. For example, Haskell (1935, 1936), using a Newtonian viscous half-space earth model with a constant density and viscosity, inferred an 'effective' (and now classic) viscosity value near 10^{21} Pa s (10^{22} poise in cgs units). In contrast, Van Bemmelen & Berlage (1935), following a suggestion by Daly (1934), argued for a model in which flow is confined to a thin (~100 km) low viscosity (~1.3×10^{19} Pa s) asthenospheric channel.

Many similar analyses followed (e.g. Vening-Meinesz 1937; Niskannen 1939; Gutenberg 1941), however, the next fundamental step arose from the studies of McConnell (e.g. 1968). McConnell used the same planar Earth geometry as his predecessors but incorporated an elastic layer overlying the viscous half-space (in order to model the effect of a lithosphere), and a depth dependent density and viscosity. Furthermore, he computed a relaxation spectrum from the observed Fennoscandian uplift by Hankel transforming the strandline (i.e. ancient shoreline) data collected by Sauramo (1958). In this procedure McConnell assumed that the Fennoscandian region had been in free decay (that is, load free) for approximately the last 9 kyrs, that each wavenumber in the response spectrum had a *single* decay time associated with it (those decay times served as the 'data' in his analysis), and that the deformation induced by the ancient Fennoscandian ice complex extended laterally no further than about 800 km from the centre of uplift. The latter assumption effectively ignored the dynamics of the peripheral bulge region, and rendered the decay times computed for the low harmonic degrees ($\ell < 14$) suspect (Parsons 1972; Cathles 1975).

McConnell (1968) argued that an elastic layer with a thickness of 120 km and a rigidity of 6.5×10^{10} Nm^{-2} (or, equivalently, a flexural rigidity of 2.5×10^{25} Nm) could explain the observed systematic decrease in relaxation time for wavelengths less than approximately 1200 km in the uplift spectrum (which the simple models of Haskell could not reconcile). Furthermore, the viscosity model he inferred was characterized by the following features: below the elastic lithosphere the viscosity diminished from 4.1×10^{20} Pa s, between 120 and 220 km depth, to 2.7×10^{20} Pa s between 220 and 400 km depth. In the next 800 km the viscosity increased from 10^{21} Pa s (between 400 and 800 km depth) to 2×10^{21} Pa s (between 800 and 1200 km depth). Below 1200 km depth the viscosity increased to 6.85×10^{21} Pa s. McConnell (1968) found that the Fennoscandian uplift data were themselves insensitive to the viscosity profile below about 1500 km depth, and he invoked independent arguments based on the apparently large non-hydrostatic bulge of the Earth deduced by Munk & MacDonald (1960) to suggest that the viscosity increased by several orders of magnitude in the deep mantle. Subsequent work by Goldreich & Toomre (1969), which showed that the excessive bulge was a numerical artefact, invalidated this argument.

Each of the analyses described above assumed that the approximation of a planar geometry would be adequate when considering the deformation due to the melting of the Fennoscandian ice complex. Once data connected with the much more massive Laurentide ice sheet, which covered all of Canada and much of the north eastern US, became available (e.g. Walcott 1972), the necessity of incorporating the influence of spherical geometry became unarguable. Indeed, spherically symmetric, self gravitating, visco-elastic Earth models were soon devised (Cathles 1971, 1975; Peltier 1974).

In his analysis Cathles (1971, 1975) argued that the purely viscous and elastic equations of motion could be assumed to decouple. In this case a solution of the resulting system of equations can be generated by solving, at each time step, the elastic and viscous equations in turn. Peltier (1974), on the other hand, invoked the correspondence principle to solve for the Laplace transform domain response of a Maxwell visco-elastic body, and then inverted this response into the time domain. Peltier (1976, 1985) showed that the time-domain response could be accurately represented using a normal mode formalism; for realistic Earth models the response, at each spherical harmonic degree, was shown to

be well approximated by a finite set of exponentially decaying modes of 'viscous gravitational relaxation'.

Cathles (1975) analysed the Fennoscandian uplift spectrum derived by McConnell (1968) using both spherical- and flat-Earth geometries, and his conclusions indicated significant non-uniqueness in the viscosity inference from this region. As an example, Cathles' (1975) preferred earth model consisted of a lithosphere with a flexural rigidity of 5×10^{24} Nm and a 75 km thick low viscosity zone (LVZ) in which the viscosity was 4×10^{19} Pa s overlying a mantle with a uniform viscosity of 10^{21} Pa s. Furthermore, he found that an Earth model with a sufficiently rigid lithosphere (e.g. 5×10^{25} Nm) would require no LVZ to fit the same data set. Clearly, large viscosity increases below 200 km depth, as inferred by McConnell, were not required to fit the uplift spectrum.

Cathles (1975) also analysed the actual observed uplift in central Fennoscandia over the last 8000 yr, as well as the average rate of vertical deflection during the last 1000 yr along a profile extending outward from the ancient Fennoscandian ice-load centre. He concluded that the model preferred on the basis of the uplift spectrum also provided a satisfactory fit to these data. A comparable fit was also possible using the channel flow model of Van Bemmelen & Berlage (1935) (although that model was much less successful in fitting the uplift spectrum). Cathles (1975) suggested that accurate data constraining the dynamics of the glacial forebulge at the periphery of the central region of uplift, which were not available to him, might allow one to distinguish between his preferred model and the channel-flow model.

In a more recent analysis Fjeldskaar & Cathles (1991) have examined shoreline tilting histories at locations near the edge of the ancient Fennoscandian ice sheet as well as the present day uplift and subsidence pattern in the region. They have argued that the data is best fit by an earth model having a lithosphere of flexural rigidity less than 10^{24} Nm (or a 'mechanical' thickness of 50 km), a 75 km thick sublithospheric low-viscosity zone (1.3×10^{19} Pa s) and a mantle of viscosity 10^{21} Pa s. In contrast, Lambeck, Johnston & Nakada (1990) have argued that Holocene sea-level changes in northwestern Europe require a lithosphere of thickness between 100–150 km, an upper mantle viscosity (that is, above the 670 km seismic discontinuity) of between $3–5 \times 10^{20}$ Pa s and a lower mantle viscosity in the range $2–7 \times 10^{21}$ Pa s. The models of Fjeldskaar & Cathles (1991) and Lambeck *et al.* (1990) are characterized by flow which is not confined to a thin channel, but rather which extends into the lower mantle region, the latter less so than the former.

All of the inferences of mantle viscosity described above have been based upon solutions of forward or direct problems of glacial isostatic adjustment. That is, the viscosity profile in the Earth model has been discretized into some small number of uniform layers and the value of the viscosity in these layers has been varied until some 'misfit' criterion has been satisfied. It is of course impossible, using such methodology, to derive rigorous error bounds on any preferred viscosity model (that is, quantify uncertainty), or to assess the resolving power of the data (that is, to quantify the non-uniqueness of the inference). In order to address issues such as these one is obliged to solve a formal inverse problem.

The unpublished doctoral dissertation of Parsons (1972) represents the only attempt, to date, to apply a rigorous inversion formalism to the glacial isostatic adjustment data set. In his analysis Parsons employed the forward model of McConnell (1968) to compute the resolving power of the relaxation spectrum that McConnell (1968) had inferred from the Fennoscandian uplift data. Since the theoretical decay times are non-linear functions of the viscosity profile their resolving power clearly depends upon the profile assumed. In this respect Parsons employed a viscosity profile similar to that deduced by McConnell (1968) (though the viscosity was reduced to 10^{21} Pa s between 800 and 1200 km depth, and to 4×10^{21} Pa s below this) which he found, through forward calculations, to fit the observed uplift spectrum. He concluded that the radial resolution provided by the data set (for the assumed Earth model) varied from approximately 100 km near the base of the lithosphere to 1350 km at a target depth of 1800 km. The data had very little resolving power below this depth; a fact that was evident to McConnell (1968) only as an 'insensitivity' to deep mantle viscosity in a suite of forward calculations.

The normal mode formalism for representing the impulse response of a spherically symmetric, self-gravitating, Maxwell visco-elastic Earth developed by Peltier (1974) was extended by Peltier (1976) to consider the inverse problem. In particular Peltier (1976) derived a variational principle which yielded exact expressions for differential kernels relating arbitrary perturbations in the radial viscosity profile to the consequent perturbations in the model decay times (or eigenfrequencies). The kernels for the decay times derived by Peltier (1976) allow for the inversion of a relaxation spectrum [of which the spectrum computed by McConnell (1968) is an example] under much more general conditions (spherical, self-gravitating, visco-elastic Earth models) than does the theory developed by Parsons (1972). However, the theory has not been used previously in this application.

In this paper we will adopt the theory of Peltier (1976), within the framework of non-linear Bayesian Inference (Tarantola & Valette 1982a, b), to invert the Fennoscandian relaxation spectra derived by McConnell (1968). Our goal, in this respect, moves beyond (and indeed incorporates) estimates of the radial resolving power of the data set, to the derivation of a set of rigorous constraints which *all* models for the viscosity variation beneath Fennoscandian must satisfy. We will use these constraints to test the plausibility of a wide class of viscosity models, including those discussed above.

In a companion paper (Mitrovica & Peltier 1993) we use the constraints derived herein as a starting point in the inversion of relative sea level (RSL) curves in the vicinity of the ancient Fennoscandian ice complex. The theory required to extend the analysis of Peltier (1976) in order to consider a full waveform (RSL curve) inversion (that is, the inversion of a data set dependent on the excitation of normal mode amplitudes, as well as on the decay times) has only recently been described (Mitrovica & Peltier 1991). An important point to note is that the inversions of RSL data are complicated by the need to explicitly consider errors in the deglaciation (i.e. surface load) chronology. The relaxation spectrum is independent of the surface loading history (theoretical predictions are based on the solution of the

homogeneous problem) and thus the analysis described in this study suffers from no such complication. Therefore, the inversions described here have the potential of providing particularly robust constraints on mantle rheology.

2 MATHEMATICAL FORMULATION

2.1 The forward problem

Following Peltier (1974) we apply the correspondence principle to solve for the Laplace-transform domain-impulse response of a radially stratified, self-gravitating, Maxwell visco-elastic planet. In the time domain this impulse response can be represented in terms of visco-elastic surface-load Love numbers of the form

$$h_\ell = h_\ell^E \delta(t) + \sum_{k=1}^{K} r_k^\ell \exp(-s_k^\ell t)$$

and (1)

$$k_\ell = k_\ell^E \delta(t) + \sum_{k=1}^{K} r_k'^\ell \exp(-s_k^\ell t)$$

where h_ℓ and k_ℓ represent the coefficients of degree ℓ in the Legendre polynomial expansions of the Green functions for, respectively, the (non-dimensionalized) radial displacement, and the gravitational potential perturbation on the earth's undeformed surface due to internal mass redistributions. At each spherical harmonic degree the Love numbers are characterized by an immediate elastic response (note the superscript E and the delta function time dependence) followed by a non-elastic response comprised of a finite set of normal modes of pure exponential decay (Peltier 1976). These modes of 'viscous gravitational relaxation', as they have been termed, are specified by the modal amplitudes (r_k^ℓ, $r_k'^\ell$) and inverse decay times or (imaginary) eigenfrequencies (s_k^ℓ), within which the dependence on the radial viscosity profile of the earth model is embedded.

Given an observed response spectrum of the type computed by McConnell (1968) using the Fennoscandian strandline data (that is, decay times versus harmonic degree) the associated forward problem requires only the determination of the modal decay times s_k^ℓ for any assumed earth model. In this study we use the procedure outlined by Peltier (1976) for the computation of these decay times.

2.2 The inverse problem

The computed relaxation spectrum is a non-linear function of the radial viscosity profile of the Earth model, and, traditionally, inversion algorithms applied to the corresponding observational data set have proceeded by linearizing the foward equations about a chosen starting model (e.g. Backus 1988). The linearization yields a system defined by a 'residual' observational data set (or misfit) and a corresponding set of Fréchet (or sensitivity) kernels which relate perturbations in the response to perturbations in the starting model. Fully non-linear inversions have been described (Tarantola & Valette 1982a, b); however, these methods also require the evaluation of Fréchet kernels when a large number of forward problems cannot be solved (as is certainly the case in the present study). In this section we will very briefly outline the theory required for the evaluation of these kernels for the relaxation spectrum data set to be inverted in subsequent sections. We will furthermore briefly discuss the Bayesian formulation to be used to perform the inversions.

2.2.1 *Fréchet kernels for the inverse decay times*

Peltier (1976) derived a variational principle which yielded the Fréchet kernels for the inverse decay times, s_k^ℓ, directly. If we define these kernels as $Z_k^\ell(v, r)$, then they satisfy the relation (see Peltier 1976, for details):

$$\frac{\delta s_k^\ell}{s_k^\ell} = \int_{\mathrm{CMB}}^{a} Z_k^\ell(v, r) \frac{\delta v(r)}{v(r)} r^2 \, dr \tag{2}$$

for small perturbations in the viscosity profile $v(r)$. The integration in eq. (2) extends from the core–mantle boundary (CMB) to the surface of the planet ($r = a$). The equation can also be written in the equivalent logarithmic form (Peltier 1976):

$$\delta \log s_k^\ell = \int_{\mathrm{CMB}}^{a} Z_k^\ell(v, r) \, \delta \log v(r) r^2 \, dr. \tag{3}$$

Mitrovica & Peltier (1991) found, using the logarithmic parameterization of eq. (3) that the kernels $Z_k^\ell(v, r)$ were capable of predicting perturbations in the logarithm of the decay times to within 10–20 per cent for a full order of magnitude change in the radial viscosity profile. As a consequence, and given the potentially large variations in viscosity in the earth's mantle, Mitrovica & Peltier (1991) chose to invert their synthetic RSL and gravity data for the logarithm of the radial viscosity profile. We adopt the same parameterization *throughout* this study, and expect that the inverse problem so described will be rendered weakly non-linear in consequence (see Tarantola & Valette 1982b; Jackson & Matsu'ura 1985, for a discussion of the implications of this point).

The kernels $Z_k^\ell(v, r)$ are characterized by two important properties (Peltier 1976):

$$Z_k^\ell(v, r) \leq 0 \tag{4a}$$

and

$$\int_{\mathrm{CMB}}^{a} Z_k^\ell(v, r) r^2 \, dr = -1. \tag{4b}$$

The relation (4a) indicates, as one might expect, that an arbitrary positive perturbation in the radial viscosity profile will necessarily lead to a decrease in the inverse decay times s_k^ℓ of *any* Earth model. Furthermore, the Fréchet kernels are normalized (eq. 4b) such that an order of magnitude increase in the viscosity profile at all depths will lead to an order of magnitude decrease in every inverse decay time.

2.2.2 *Non-linear Bayesian inference*

Following Mitrovica & Peltier (1991) we will formulate the non-linear inversion of the relaxation spectrum as a problem in Bayesian inference. The application of Bayesian inference to geophysical inverse problems has been described by many authors (Backus 1971, 1988; Tarantola & Valette 1982a,b; Jackson & Matsu'ura 1985). The Bayesian philosophy provides an algorithm for combining defensible *a priori*

information regarding the model parameters (in the present case the logarithm of viscosity in a radially discretized form) with the observational data to yield an *a posteriori* state of information (Backus 1988).

In the event that a very large number of forward problems cannot be solved, Tarantola & Valette (1982b) have shown, when both the prior beliefs and observation errors are normally distributed, that the maximum likelihood estimate of the posterior distribution can be found by solving the following iterative equation:

$$\hat{\mathbf{X}}_{k+1} = \hat{\mathbf{X}}_k + (\mathbf{F}_k^T \mathbf{V}_\xi^{-1} \mathbf{F}_k + \mathbf{V}_{\mathrm{PR}}^{-1})^{-1} \times \{\mathbf{F}_k^T \mathbf{V}_\xi^{-1} [\mathbf{y} - f(\hat{\mathbf{X}}_k)] - \mathbf{V}_{\mathrm{PR}}^{-1} (\hat{\mathbf{X}}_k - \mathbf{X}_{\mathrm{PR}})\} \quad (5)$$

where $\mathbf{y}$ is the observational data set, $\mathbf{V}_\xi$ is the covariance matrix of the data errors (which are assumed to have a zero mean), $\mathbf{X}_{\mathrm{PR}}$ and $\mathbf{V}_{\mathrm{PR}}$ are the prior model and covariance matrices, $\hat{\mathbf{X}}_k$ is the kth model iterate ($\hat{\mathbf{X}}_0$ is the starting model), $\mathbf{F}_k$ is a matrix whose rows are the Fréchet kernels (in their discretized form and scaled by $r^2 dr$ in accord with eq. 3), and $f(\hat{\mathbf{X}}_k)$ represents a non-linear forward prediction using the model $\hat{\mathbf{X}}_k$. Since the errors are assumed to be normally distributed, the iteration will be considered to have converged when the statistic Q, defined by

$$Q(\hat{\mathbf{X}}_k) = [\mathbf{y} - f(\hat{\mathbf{X}}_k)]^T \mathbf{V}_\xi^{-1} [\mathbf{y} - f(\hat{\mathbf{X}}_k)] \quad (6)$$

is within the 95 per cent confidence interval of the χ^2_N distribution (where N is the number of data points).

In weakly non-linear inverse problems Tarantola & Valette (1982b) and Jackson & Matsu'ura (1985) have argued that the posterior covariance matrix of the model parameters can be approximated by

$$\mathbf{V}_{\mathrm{PO}} = [\mathbf{F}^T \mathbf{V}_\xi^{-1} \mathbf{F} + \mathbf{V}_{\mathrm{PR}}^{-1})^{-1} \quad (7)$$

where the matrix of Fréchet kernels is evaluated at the posterior model. Following the arguments of Tarantola & Valette (1982b), the resolving power of the data at the ith target will be assessed by examining the pattern of covariances along the ith row of $\mathbf{V}_{\mathrm{PO}}$.

3 RESULTS AND DISCUSSION

The data to be inverted in this section are the logarithms of the inverse decay times (see the left hand side of eq. 3), at various spherical harmonic degrees, inferred from the isostatic adjustment pattern in Fennoscandia. As discussed in the introduction, McConnell (1968) derived a relaxation spectrum (that is, a spectrum of decay times as a function of wavelength) for Fennoscandia using a large set of strandline data collected by Sauramo (1958) along a profile extending from Angermanland, Sweden, to near Izhora in Russia. In particular, McConnell (1968) focused on six sets of shoreline features of different ages (YOLDIA I, YOLDIA VI, Echineis Sea, Ancylus Lake, Mastogloia Sea and Litorina Sea, of ages, respectively, 9800, 9200, 8800, 8000, 8000 and 6000 yr). The derivation of the relaxation spectrum from the sea shoreline features proceeded in three main steps (see McConnell 1968, for details). First, Sauramo's (1958) shoreline levels were corrected for the effects of sea-level fluctuations by 'subtracting the elevation of the untilted portion from the elevation of all other portions of the same shoreline'. This procedure, with suitable extrapolation, yielded 'reduced beach levels' over a 800 km profile (sampled every 36 km) for each of the shoreline features named above (see McConnell 1968; Fig. 3). In the second step of the procedure McConnell Hankel transformed each of the six profiles to generate an equal number of transformed shoreline elevations (that is, an amplitude versus wavenumber plot for each of the six shorelines; see McConnell 1968, Fig. 4). Finally, for any particular wavenumber, a characteristic relaxation time could be inferred by fitting an exponential form through the six (or some subset of the six) amplitudes of known age.

McConnell (1968) believed that the most accurate relaxation times were derived using the five youngest beaches (that is, excluding the 9800 year-old YOLDIA I beach). He argued that the derivation would thus incorporate almost all of the available data, and avoid shorelines formed at a time when the central Fennoscandian region might still have been covered by ice. The two spectra he derived using the five youngest beaches and all six beaches diverged above wavenumbers of $4 \times 10^{-6}\,\mathrm{m}^{-1}$ (or spherical harmonic degrees above 25) where the former exhibited consistently shorter relaxation times (see McConnell 1968, Fig. 5). If the time period extending from the formation of the YOLDIA I beach to the YOLDIA VI beach incorporated some melting of remnant ice cover, then elastic effects in the uplift should, in contrast, cause relaxation times inferred from all six beaches to be shorter than those derived excluding YOLDIA I. This implies that the entire period subsequent to the formation of YOLDIA I was probably characterized by free decay. Regardless of whether the five largest or all six beaches were used in the derivation of the relaxation spectrum, McConnell (1968) found that reliable relaxation times (as measured by the level of success obtained in the fitting of exponential forms through the transformed shoreline elevations) could not be obtained for wavenumbers between 8×10^{-6} and $10^{-5}\,\mathrm{m}^{-1}$ (or degrees between 50 and 64).

Sauramo's (1958) data set of strandline levels were not published with error bars, and hence it is impossible to ascribe a formal uncertainty to McConnell's (1968) relaxation spectra (indeed, McConnell did not do so). This difficulty is reinforced by potential systematic errors introduced in McConnell's beach-level reduction procedure (see McConnell 1968). To generate reasonable, and conservative, error estimates we have adopted the following Monte Carlo procedure. As a basic data set we begin with McConnell's set of six reduced beach level profiles. Rather than Hankel transform this set of beaches, as McConnell did, we add Gaussian-distributed random noise to each data point on the various profiles, and then Hankel transform the result. From the transformed beach levels we then best-fit the required exponential form to derive a relaxation time. These relaxation times where computed for spherical harmonic degrees between 14 and 80 inclusive. The full procedure was repeated 10^5 times to generate 10^5 realizations of the relaxation spectrum, and from these the statistics of the relaxation spectrum was determined (as described below).

The 10^5 evaluations of the relaxation spectrum were partitioned so that half were generated using the five youngest beaches, and the remainder generated using all six beaches. Furthermore, following McConnell (1968), any

estimated relaxation time was considered acceptable only if it yielded an RMS deviation between the observed (that is, transformed shoreline elevations) and theoretical (that is, exponential form) uplift of less than 20 per cent of the transformed present-day height of the oldest shoreline used (either YOLDIA I or VI). In accord with McConnell's (1968) results, we have found that few, if any, relaxation times for spherical harmonic degrees between 46 and 64 satisfied this criterion, and hence relaxation times in this degree range are left unconstrained.

In the absence of direct guidelines, the statistics of the random errors added to McConnell's (1968) reduced beach levels were chosen on the basis of characteristic error levels associated with land-based surveys. Tushingham (1989), in his analysis of relative sea-level histories in Hudson Bay, has estimated an uncertainty in elevation to be ±15 per cent (representing ± two standard deviations of error) with a minimum error of ±1 m due to instrument error and tides. To be even more conservative we have chosen to add random errors with a standard deviation equal to 10 per cent of the reduced beach level.

Let us say that at spherical harmonic degree ℓ there are $N(\ell)$ estimates of the logarithm of the inverse relaxation time $[N(\ell) \leq 10^5]$ which satisfy the acceptance criterion discussed above. The mean, standard deviation, and covariance of these estimates can be computed in a straightforward manner using the usual formulii of sampling theory. The vector $\mathbf{y}$ and the matrix $\mathbf{V}_\xi$ appearing in eqs (5) through (7) are thus determined.

The shaded region on Fig. 1 represents the $\pm 1\sigma$ error bounds on the relaxation spectrum generated from our Monte Carlo procedure. Notice that in spite of the substantial errors we have ascribed to McConnell's set of reduced beach levels, the relaxation spectrum remains significantly constrained. For spherical harmonic degrees 14 through 30 the decay time is approximately 3 to 4 kyr. In contrast, at the largest degrees (smallest wavelengths), the decay time ranges from 1–2 kyr. As discussed, there are no relaxation time estimates between degrees 46 and 64.

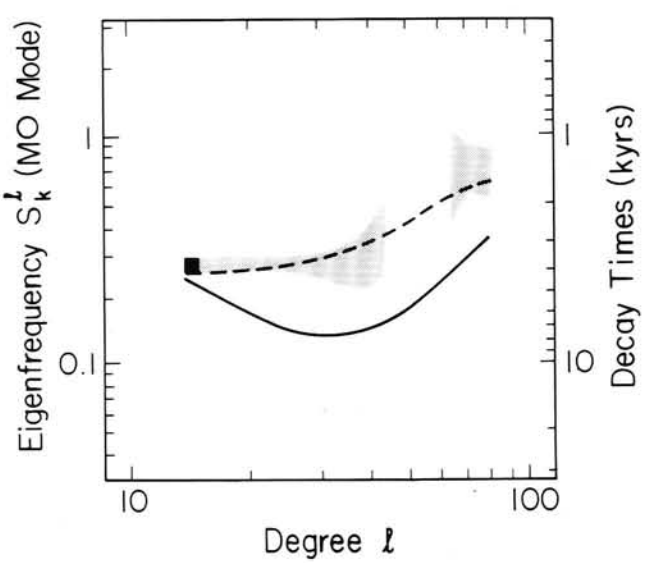

Figure 1. Shaded region: relaxation spectrum (including a $\pm 1\sigma$ uncertainty) inferred from the post-glacial uplift of central Fennoscandia (after McConnell 1968) for spherical harmonic degrees ranging from 14 to 45 and 65 to 80 (see text). The solid line is the relaxation spectrum computed for the isoviscous model A specified in Table 1 (with a 120 km elastic lithosphere), while the dashed line is the spectrum computed for the *a posteriori* model of inversion no. 1 (Fig. 3a, solid line; see also Table 2).

Although McConnell's (1968) derivation of decay times extended to degrees as low as 10 we concur with both Parsons (1972) and Cathles (1975) who have argued that the data for the lowest degrees ($\ell < 14$) may be inaccurate due to McConnell's assumption that the post-glacial deformation extended no further than 800 km from the centre of uplift (the Angermanland region of Sweden). We have assumed, as did McConnell (1968), that the response at each spherical harmonic degree was characterized by a single decay time (i.e. $K = 1$ in the summations of eq. 1). Fortunately, for the degree range considered in this section ($\ell \geq 14$) the fundamental mode of relaxation (termed the MO mode; see, for example, Peltier 1976, Mitrovica & Peltier 1991) generally carries appreciably more than 90 per cent of the total modal strength.

The earth models used in this study have an inviscid core and an elastic lithosphere (whose thickness may be varied). The radial distance from the earth's centre to its surface is discretized using 161 layers in our numerical formulation, 66 of which define the core and 65 the lower mantle. The term 'model' used in this section (and section 2.2.2) refers to the logarithm of viscosity in each of the approximately 90 layers within the lower mantle and upper mantle below the lithosphere (the exact number of layers depends on the lithospheric thickness). We will examine inversions using three different prior ($\mathbf{X}_{\mathrm{PR}}$ in eq. 5) and starting ($\hat{\mathbf{X}}_{k=0}$ in eq. 5) models chosen from the models A, B, and C summarized in Table 1. In this section the individual elements of the prior model vector will be assumed to be totally uncorrelated (that is, no *a priori* assumption of smoothness in the model will be made except on the order of the individual layer thickness). Furthermore, with only a single exception (inversion no. 2 below) these parameters will *all* have a variance of 1.0 assigned to them. Thus the matrix $\mathbf{V}_{\mathrm{PR}}$ will generally be the identity matrix. As a consequence, and as an example, this yields 95 per cent confidence intervals of (19.845, 23.845) in the lower mantle and (19.0, 23.0) in the upper mantle for prior model B. Finally, inversions will be performed for models with lithospheric thicknesses ranging from 70 to 145 km.

Prior to discussing the inversions performed on the relaxation spectrum of Fig. 1 it will be instructive to examine the Fréchet kernels (Z_k^ℓ, in eq. 3, for the fundamental mode of relaxation) for the data set. As an example, the kernels for spherical harmonic degrees $\ell = 14$, 30, 45, and 70, computed using the mantle model A (Table 1) and a 120 km

Table 1. Mantle models.

	A	B	C
Lower Mantle	21.0	21.845	21.0
Upper Mantle*	21.0	21.0	20.7

*below elastic lithosphere

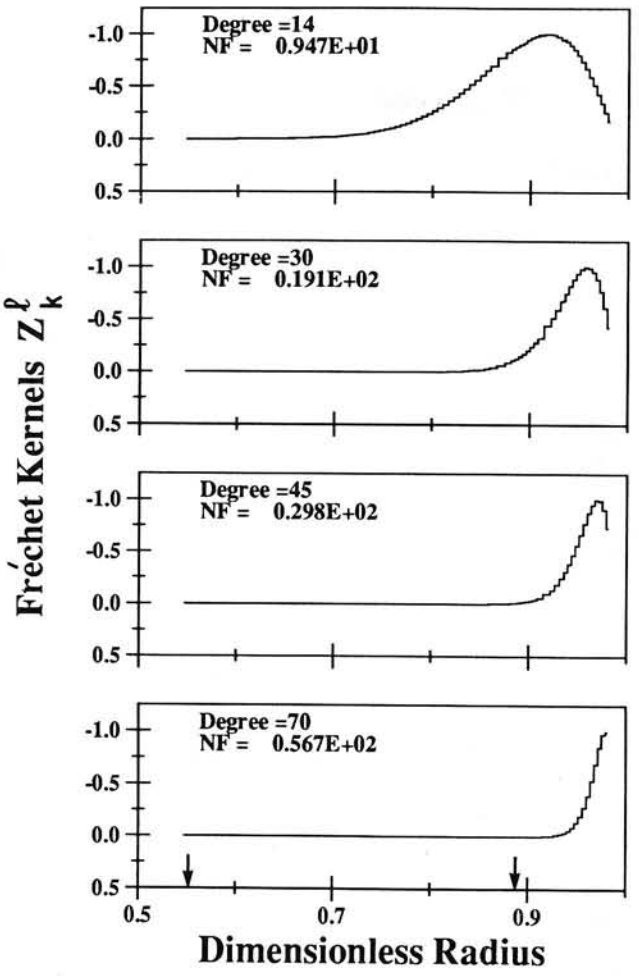

Figure 2. Fréchet kernels, Z_k^ℓ (eq. 3), for the inverse decay times of the fundamental (MO) mode of viscous gravitational relaxation, computed using the isoviscous Earth model A (Table 1) with a 120 km lithosphere. The kernels for four different spherical harmonic degrees (as labelled) are shown on the figure, and each is normalized (by the factor NF) to yield a peak value of −1.0. The abscissa scale is non-dimensionalized using the earth's radius, and the arrows at left and right on the bottom frame refer to the value at the CMB and at 670 km depth, respectively.

lithosphere, are plotted on Fig. 2. Not surprisingly, as the spherical harmonic degree is increased, the peak in the kernels (and thus the region of peak sensitivity for the computed inverse decay time) sweeps to shallower depths; so that while at degree 14 it occurs at a depth of 600 km, by degree 45 it has reached near the base of the lithosphere. Of course this has fundamental implications for any inference of mantle viscosity based on the data set. It implies that the relaxation spectrum data set of Fig. 1 provides little information regarding mantle rheology below about 1300 km depth in the earth.

A total of 9 different inversions were performed on the relaxation spectrum described above and illustrated in Fig. 1. Table 2 summarizes the inputs defining these inversions (the prior model and its variance, the starting model and the lithospheric thickness) as well as a few summary statistics which will be defined and discussed below. All nine inversions were found to satisfy the convergence criteria (6) in a *single* iteration, indicating that an assumption of quasi-linearity is extremely accurate in these cases (Peltier 1976; Mitrovica & Peltier 1991).

To begin let us consider inversion no. 1, for which the isoviscous mantle model A (Table 1) was chosen as both the prior and starting model, the prior model covariance matrix was the identity matrix, and the lithosphere was constrained to have a thickness of 120 km (for this inversion, and inversion no. 2, the Fréchet kernels shown on Fig. 2 are those used in the initial application of eq. 5). The *a posteriori* model for inversion no. 1 (that is the solution of eq. 5 which satisfies the convergence criterion on eq. 6) is given by the solid line on Fig. 3. (The relaxation spectra computed using the *a priori* and *a posteriori* models are given by, respectively, the solid and dashed lines on Fig. 1; the latter clearly satisfies the observational constraint). The prior (and starting) model for inversion no. 1 is specified by the horizontal dashed line on Fig. 3. An important characteristic of the inversion, and one shared with all subsequent inversions to be discussed in this section, is that the *a posteriori* model tends toward the prior model in the deep mantle. This is a reflection of the fact that the relaxation-spectrum data set provides little information regarding the viscosity of the earth's mantle below 1300 km depth (see Fig. 2) and hence the *a posteriori* state of knowledge is dominated by the prior state. In contrast, in the top half of the mantle the *a posteriori* state of knowledge seems, apparently, to be fundamentally altered from the prior state of knowledge by the inclusion of the information provided by the observational data set. Of course, the significance of the variations apparent in the *a posteriori* model need to be assessed by considering both the errors and resolving power associated with the inference.

On Fig. 4 we have plotted the *a posteriori* value of the variance of the individual model parameters (that is the diagonal elements of the matrix $\mathbf{V}_{PO}$, given by eq. 7, computed at the *a posteriori* model $\mathbf{X}_{PO}$) versus depth in the mantle. Recall (see Table 2), the prior variances are all 1.0, and thus the curve on Fig. 4 may also be interpreted as the *ratio* of the *a posteriori* to *a priori* variances. We will emphasize the latter interpretation of Fig. 4. Following Tarantola & Valette (1982b) and Backus (1988), a model parameter is said to be 'resolved' by the data when the *a posteriori* variances are substantially smaller than the *a priori* variances (that is when the ratio is small). Clearly none of the model parameters below about 1300 km depth (0.8 dimensionless radius units) are resolved by the data, which is not surprising given that the relaxation spectrum data are not sensitive to the rheology in this region of the mantle (Fig. 2). In contrast, at shallower depths the ratio generally, though not monotonically, tends toward smaller values. It is interesting to note, however, that the ratio is never substantially smaller than 1.0 (its minimum value is near 0.6 in the sublithospheric region; however, it generally exceeds 0.8), which indicates that the data are not able to resolve rheological structure on a radial length scale comparable to the layer widths. In this case it is more interesting to consider the ratio of the *a posteriori* to *a priori* variances of the average value of the model parameters in some more extensive region of the mantle (Jackson 1979; Mitrovica & Peltier 1991). We will show below that when the regions are chosen to be consistent with the resolving

Table 2. Inversions.

		1	2	3	4	5	6	7	8	9
INPUTS										
X_{PR}		A	A	A	A	B	C	A	A	A
$\{V_{PR}\}_{ii}$		1.0	2.0	1.0	1.0	1.0	1.0	1.0	1.0	1.0
$\hat{X}_{t=0}$		A	A	B	C	B	C	A	A	A
LT (km)		120	120	120	120	120	120	70	100	145
SUMMARY STATISTICS										
<1>	PR	21.00 ± .23	21.00 ± .33	21.00 ± .23	21.00 ± .23	21.48 ± .23	20.87 ± .23	21.00 ± .23	21.00 ± .23	21.00 ± .23
	PO	21.02 ± .08	21.01 ± .12	20.88 ± .08	20.92 ± .08	20.93 ± .13	20.93 ± .08	21.03 ± .10	21.03 ± .09	20.99 ± .08
<2>	PR	21.00 ± .25	21.00 ± .35	21.00 ± .25	21.00 ± .25	21.00 ± .25	20.70 ± .25	21.00 ± .25	21.00 ± .25	21.00 ± .25
	PO	20.69 ± .08	20.66 ± .12	20.65 ± .08	20.60 ± .08	20.60 ± .08	20.58 ± .08	20.74 ± .08	20.70 ± .08	20.66 ± .08
<3>	PR	21.00 ± .42	21.00 ± .58	21.00 ± .42	21.00 ± .42	21.00 ± .42	20.70 ± .42	21.00 ± .36	21.00 ± .38	21.00 ± .46
	PO	20.58 ± .21	20.55 ± .30	20.58 ± .21	20.50 ± .22	20.54 ± .26	20.50 ± .21	20.15 ± .16	20.39 ± .19	20.73 ± .23
ρ_{12}	PR	0.50	0.50	0.50	0.50	0.50	0.50	0.50	0.50	0.50
	PO	0.06	-0.17	0.10	0.06	0.06	-0.05	-0.19	0.14	0.06
ρ_{13}	PR	0.0	0.0	0.0	0.0	0.0	0.0	0.0	0.0	0.0
	PO	-0.04	-0.03	0.10	-0.04	0.04	-0.02	0.01	-0.09	0.02
ρ_{23}	PR	0.11	0.11	0.11	0.11	0.11	0.11	0.09	0.10	0.13
	PO	0.10	0.11	0.06	0.10	0.09	0.10	-0.03	0.08	0.09

$\mathbf{X}_{PR}$ Prior model (see Table 1).
$\{\mathbf{V}_{PR}\}_{ii}$ Diagonal elements of prior covariance matrix. Non-diagonal elements are zero. $\mathbf{V}_{PR} = \{\mathbf{V}_{PR}\}_{ii}\mathbf{I}$ (I is the identity matrix).
$\hat{\mathbf{X}}_{t=0}$ Starting model (see Table 1)
LT Lithospheric thickness.
$\langle i \rangle$ Volumetric average of model parameters in region i (see eq. 9). The regions are defined on Table 3.
ρ_{ij} Cross-correlation of the averages $\langle i \rangle$ and $\langle j \rangle$ (see eq. 10).

power of the data an order of magnitude reduction in the prior variance can result (see also Mitrovica & Peltier 1991).

The resolving power of the relaxation-spectrum data can be assessed from the posterior covariance matrix (Tarantola & Valette 1982b). For example, the radial extent of non-negligible off-diagonal covariances on the ith row of the covariance matrix is a measure of the resolving power of the data at the depth corresponding to that row. We have plotted on Fig. 5, 12 different rows (or target depths, TD, as labelled on each frame of the figure) of the posterior covariance matrix for inversion no. 1. In each case the curves are normalized by the amplitude of the largest off-diagonal covariance (specified by the parameter NF). In this case the diagonal element (the variance) has a (positive) value which is off the scale of the plot (it is, however, specified on Fig. 4).

The target depths sampled on Fig. 5 extend from the very deep (2885 km depth) to very shallow (195 km depth) mantle. Significantly, for target depths below 1000 km depth (the first four frames on Fig. 5) the curves peak at a layer whose depth is appreciably shallower than the target depth. Once again, this is a reflection of the very limited resolving power of the data in this deep mantle region. In contrast, at target depths shallower than 1000 km, the pattern of off-diagonal covariances is centred approximately on the target layer. In this respect it is clear that the radial extent of the non-negligible covariances diminishes (that is, the resolving power of the relaxation spectrum data set improves) monotonically as one considers targets at depths from 982 km through to 195 km.

Any quoted value of the resolving power will depend somewhat on the measure used to define a 'non-negligible' covariance. On Fig. 6 we have plotted the resolving power computed as the radial distance between layers in which the normalized covariance falls below an amplitude of 0.1 (that is less than 10 per cent of the peak off-diagonal covariance), as a function of target depth in the top 1200 km of the mantle. Using this measure, the radial resolving power of the relaxation spectrum data set improves from approximately 1200 km at a depth of 1000 km to better than 125 km at the base of the lithosphere. The *a posteriori* model for inversion no. 1 (solid line on Fig. 3) exhibits a noticeable variation across 670 km depth (the boundary between the upper and lower mantle regions) that extends approximately 350 km from peak (at 850 km depth) to trough (at 500 km depth). The results of Fig. 6 indicate that the variation should have no significance ascribed to it. In contrast, the same *a posteriori* model exhibits a low-viscosity region at the base of the lithosphere which the relaxation spectrum data set is just capable of resolving (see Fig. 6).

As discussed in the introduction, Parsons (1972) computed the resolving power of the same relaxation spectrum data set using an earth model with an elastic layer overriding a viscous half-space, and a depth-dependent

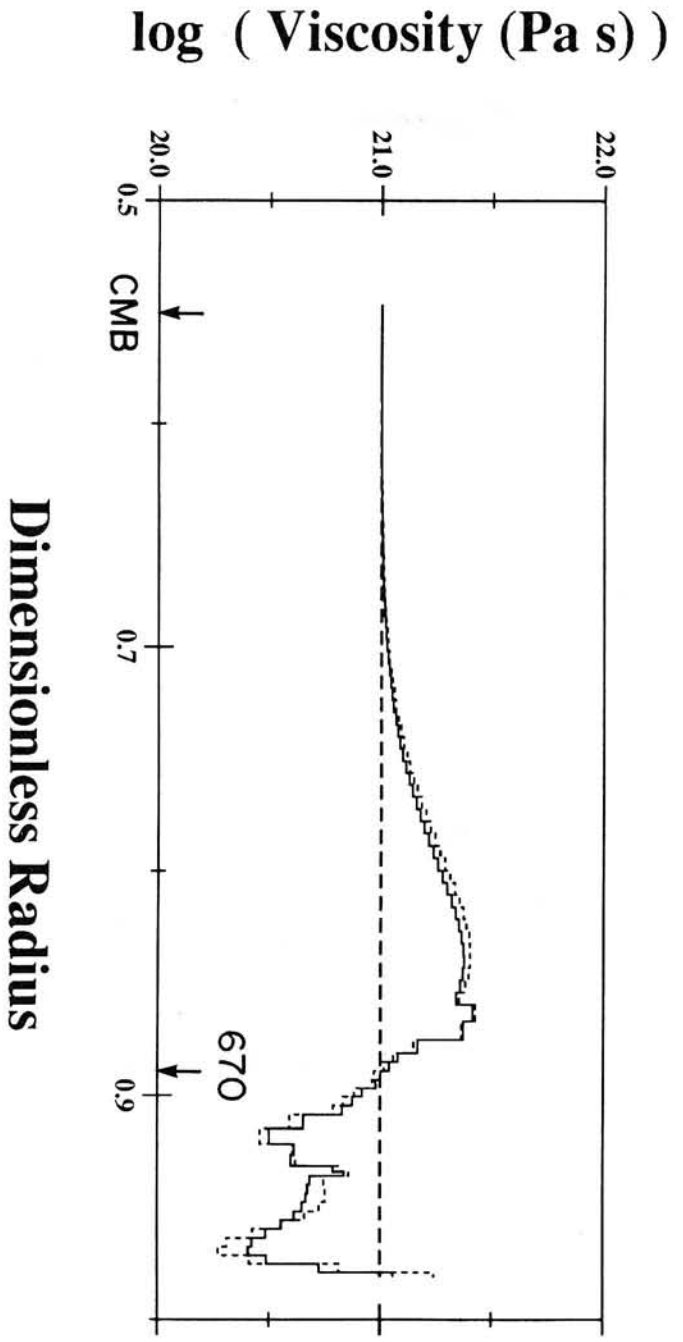

Figure 3. Results for inversion nos. 1 and 2 (see Table 2 for details) of the relaxation spectrum data set. The horizontal dashed line represents the isoviscous prior and starting model A used in the inversions, while the solid and dotted lines give the *a posteriori* models (that is the maximum likelihood estimates) of inversion nos. 1 and 2, respectively. The abscissa scale is non-dimensionalized as in Fig. 2, with the location of the CMB and the seismic discontinuity at 670 km depth specified by labelled arrows.

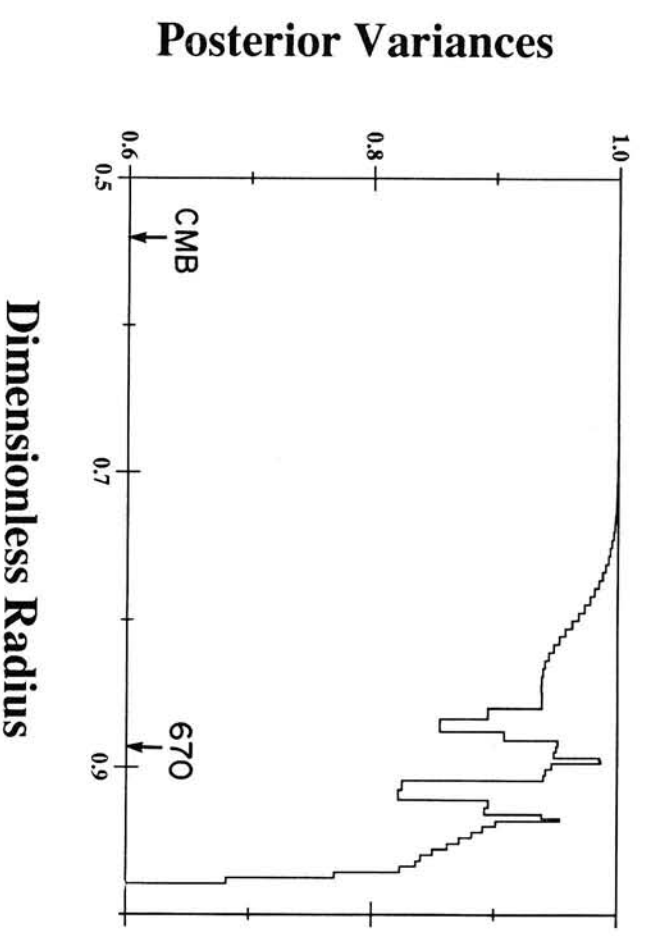

Figure 4. The *a posteriori* variances of the individual model parameters for inversion no. 1 (see Table 2 for details) as a function of dimensionless radius. The *a priori* variances of the model parameters in inversion no. 1 are all 1.0, and they would therefore lie on the top edge of the plot.

viscosity profile very similar to that inferred by McConnell (1968). The resolving kernels plotted by Parsons (1972) have a depth extent which is comparable to that exhibited by the (associated) row of the posterior covariance matrix derived in this study (Fig. 5). The measure of 'spread' adopted by Parsons (1972) (as defined in the technique of Backus & Gilbert 1968) tends to reflect the width of the resolving kernels at a much higher normalized amplitude than the value adopted here (10 per cent of the maximum value), and therefore the values quoted by Parsons (1972) are considerably smaller than those plotted on Fig. 6.

Let us consider a general linear combination of the model parameters $\mathbf{g}^T\mathbf{x}$. The *a posteriori* variance of the combination (which we denote by S^2_{PO}) must be smaller than or equal to the *a priori* variance (denoted S^2_{PR}; Tarantola & Valette 1982a), and the ratio of the two is given by

$$S^2 = \frac{S^2_{\mathrm{PO}}}{S^2_{\mathrm{PR}}} = \frac{\mathbf{g}^T\mathbf{V}_{\mathrm{PO}}\mathbf{g}}{\mathbf{g}^T\mathbf{V}_{\mathrm{PR}}\mathbf{g}} \tag{8}$$

where $\mathbf{V}_{\mathrm{PR}}$ and $\mathbf{V}_{\mathrm{PO}}$ are the *a priori* and *a posteriori* model covariance matrices. One possible choice for $\mathbf{g}$ is a vector which is zero in all but one element corresponding to a particular target depth. In this case we have found, from inversion no. 1, that the value of S^2 is not appreciably smaller than 1.0 (see Fig. 4) and have concluded that the relaxation spectrum data do not 'resolve' rheological structure on the radial length scale of the individual model layers (that is certainly also clear from the results of Figs 5 and 6). A logical choice for the $\mathbf{g}$ vector is therefore one which reflects the true resolving power of the data, and in

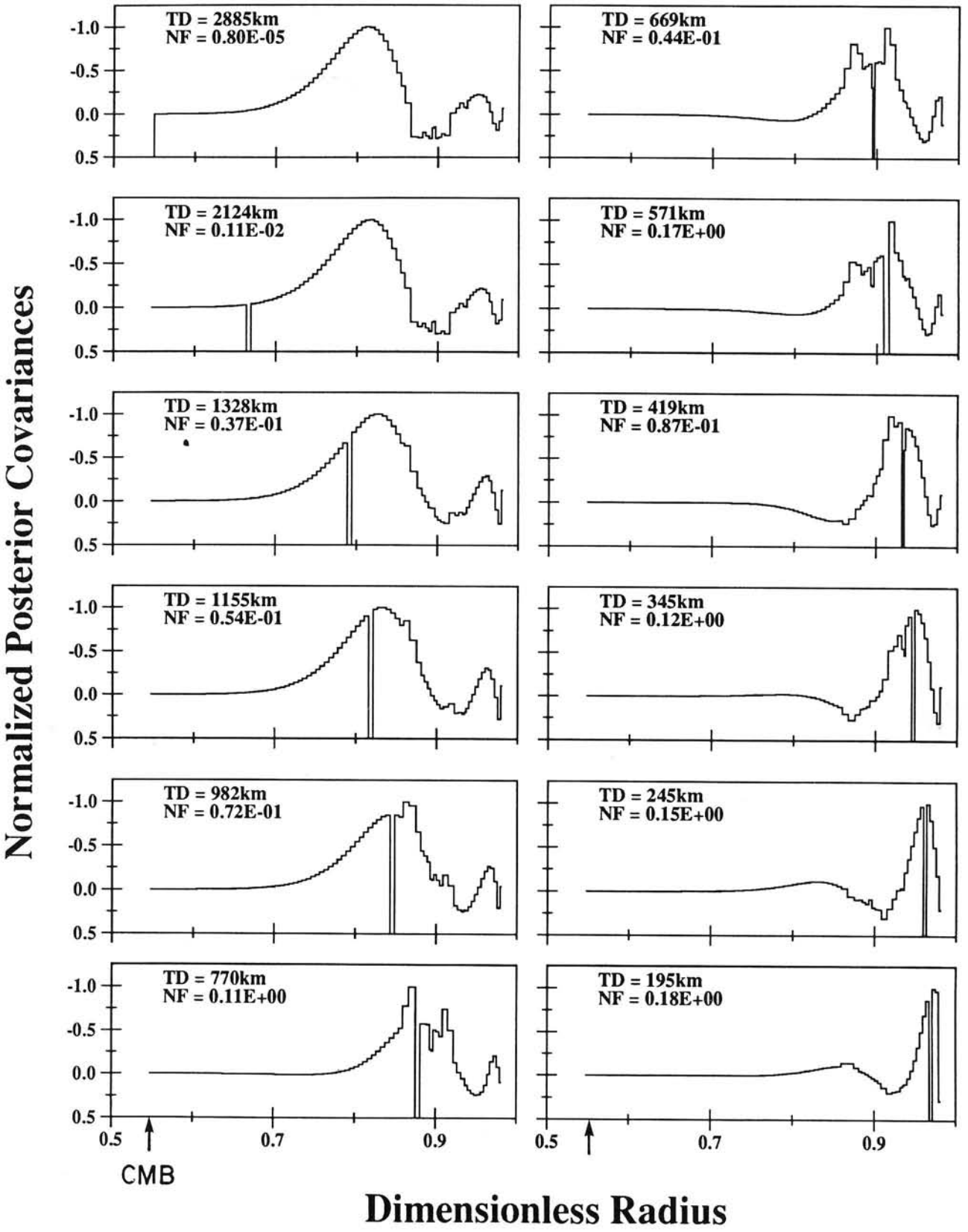

Figure 5. 12 different rows (or target depths, TD, as labelled on each frame) of the *a posteriori* model covariance matrix $\mathbf{V}_{PO}$ (eq. 7) for inversion no. 1 (see Table 2 for details). In each case the rows are normalized by the amplitude of the largest off-diagonal covariance on the row (specified by the parameter NF). The diagonal element on the row (or the variance of the model parameter associated with the target depth) is off the scale of the plot (note the sharp dip at the curves in each frame which serves to locate the target depth), however, it may be ascertained from Fig. 4. The abscissa scale is non-dimensionalized as in Fig. 2.

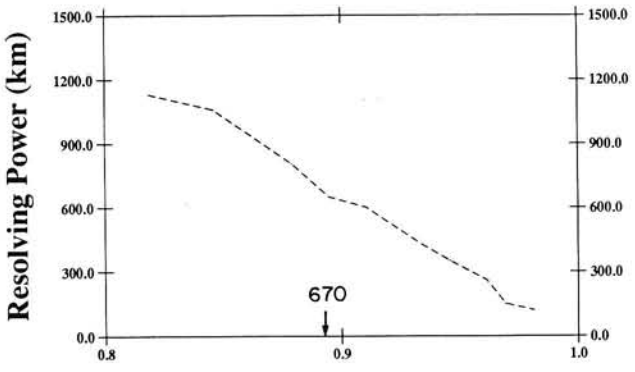

Figure 6. The resolving power of the Fennoscandian relaxation spectrum data set (in the spherical harmonic degree range 14 to 45 and 65 to 80) as a function of dimensionless radius. For a particular target depth, or model parameter, the resolving power is computed as the radial distance between model layers in which the *a posteriori* covariance with the model target parameter falls to 10 per cent of the peak covariance. The abscissa extends to a depth of approximately 1300 km (a dimensionless radius of 0.8).

this respect we may follow two courses. Backus (1988) has described a technique for finding a set of vectors $\mathbf{g}_i$, constrained such that $\mathbf{g}_i^T\mathbf{x}$ are uncorrelated both in the *a priori* and *a posteriori* state, which yield a ratio S^2 that is much smaller than 1.0. The number of such vectors, or alternatively the number of independent estimates resolved by the data, is equal to the trace of the so-called resolution matrix (Backus 1988). In the inversions described in this section this value generally lies between 3.2 and 3.8. The drawback of the procedure is that the vectors so derived generally exhibit large oscillations so that the physical interpretation of the estimate $\mathbf{g}^T\mathbf{x}$ is unclear. In this respect, Jackson (1979) and Mitrovica & Peltier (1991) have advocated the use of simple 'box-car' functions whose width is comparable to the resolving power of the data. In this case the linear combination $\mathbf{g}^T\mathbf{x}$ represents the average value of the model parameters (the logarithm of the radial viscosity profile in a discretized form) in the chosen region. The drawback, in this choice of $\mathbf{g}_i$, is that the estimates $\mathbf{g}^T\mathbf{x}$ are not necessarily uncorrelated (in either an *a priori* or *a posteriori* sense).

We will adopt the latter approach in this section, and in particular choose the vectors $\mathbf{g}_i$ which yield the *volumetric* average of the logarithm of viscosity in some region of the earth's mantle. In this case, for a region extending over a radial depth range $\mathbf{r}_1$ to $\mathbf{r}_2$, the vector $\mathbf{g}_i$ is generated from a discretized version of the expression

$$\langle \log v \rangle = \frac{\int_{r_1}^{r_2} r^2 \log v(r)\, dr}{\int_{r_1}^{r_2} r^2\, dr}. \tag{9}$$

From a consideration of the results of Fig. 5 [in particular, for target depths 669 km, 419 km, and (not shown) 130 km], we have chosen to examine three regions. The depth range which defines each region is provided on Table 3.

Table 3.

Region	Depth Range (km)
1	1040 - 400
2	670 - 210
3	235 - base of the lithosphere

It must be emphasized that the three regions listed on Table 3 are chosen on the basis of the *computed* resolving power of the data. One might be tempted, for example, to consider the average logarithm of viscosity in the transition zone (400 to 670 km depth), however, the rheology in the region is not resolved by the data, and the results will be strongly correlated with the average value of the model parameters in the 400 km region at the top of the lower mantle. Hence an inference of the average logarithm of viscosity in this region of the mantle alone can be very misleading (we will return to this point below). By considering the average over a depth range consistent with the resolving power of the relaxation spectrum data set our goal is to generate robust inferences which all proposed models of the radial viscosity variation below Fennoscandia must satisfy.

On Table 2 we have listed the computed average logarithm of viscosity in each of the three regions listed in Table 3, for inversion no. 1 (and all subsequent inversions of the relaxation spectrum data set to be discussed in this section). The symbol ⟨i⟩ denotes the average for the ith region, and the symbols PR and PO distinguish the averages computed using the *a priori* and *a posteriori* models and statistics. The quoted errors represent the associated standard deviation of the estimate (S_{PR} and S_{PO}, as defined in eq. 8, for the *a priori* and *a posteriori* state, respectively). Also listed in Table 2 are the cross correlations between the three estimates, defined as

$$\rho_{ij} = \frac{\mathbf{g}_i^T \mathbf{V}_{\mathrm{P}} \mathbf{g}_j}{(S_{\mathrm{P}})_i (S_{\mathrm{P}})_j} \tag{10}$$

where i and j represent the ith and jth region, and P stands for either PR or PO.

The errors quoted in Table 2 may be slightly misleading because they will depend on the number of layers of the numerical model which reside in the particular region of interest (Backus 1988). A more robust measure of the effect of incorporating data into the analysis, as discussed above (Jackson 1979; Backus 1988), is to consider the *ratio* of the *a posteriori* and *a priori* variances. As an example, for the average logarithm of viscosity in region no. 2, for inversion no. 1, the ratio is approximately 0.1; this represents an order of magnitude reduction in the variance of the estimate. Recall the ratio which characterized estimates of the individual model parameters was generally greater than 0.8 (Fig. 6). A second important point regarding Table 2 is that the *a posteriori* cross-correlations between the estimates for the three regions are usually quite small, and thus the estimates are generally nearly independent.

The summary statistics listed on Table 2 will serve as the

basis for the comparison of the inversions of the relaxation spectrum data set to be discussed in this section. In inversion no. 2 (dotted line, Fig. 3b) the *a priori* variances of the model parameters were increased to 2.0. A comparison of inversion nos. 1 and 2, on Table 2, indicates that the computed *a posteriori* averages are essentially unaltered, and the error bounds only slightly increased. In inversions nos. 3 and 4 we examine the effect of varying the starting model, $\hat{\mathbf{X}}_{k=0}$, on the *a posteriori* inferences. Inversion no. 3 uses starting model B (Table 1) in which the lower mantle model parameters are increased (with respect to model A) to a value of 21.845. In contrast inversion no. 4 uses starting model C, where the upper mantle model values are reduced (again, with respect to model A) to a value of 20.7. The *a posteriori* models for inversions nos. 1, 3, and 4, are plotted on Figs 7a, b and c, respectively. In each frame of the figure the *a priori* model A (used in all three inversions) is given by the solid line, while the starting model is given by the dashed line. Clearly, the inversions have converged to very similar *a posteriori* models. Once again, this convergence is reflected in the summary statistics of Table 2, where the difference between the inferences based on the inversions are insignificant.

Inversions nos. 1 through 4 have all used the same isoviscous *a priori* model A. In order to investigate the effect of varying the *a priori* beliefs inversions nos. 5 and 6 were performed using the *a priori* (and starting) models B and C, respectively. The *a posteriori* models for inversions 1, 5 and 6 are given on Fig. 8. As discussed in the context of Fig. 3, the *a posteriori* models of Fig. 8 all tend toward their

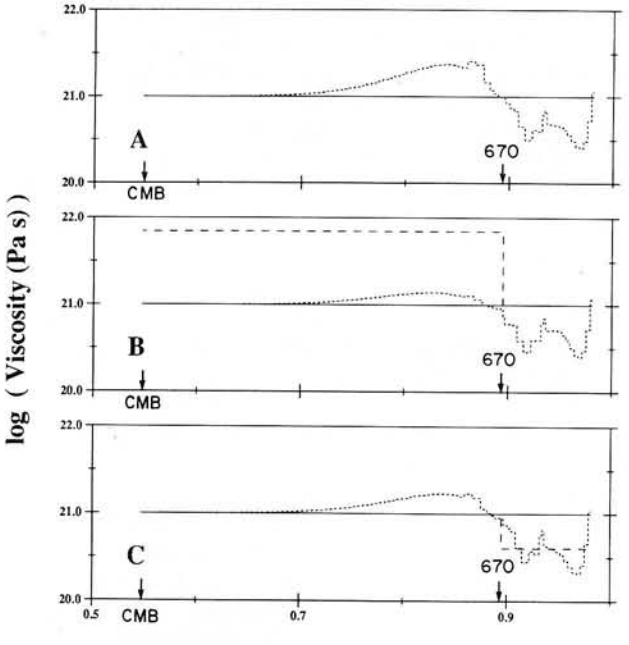

Figure 7. The results for inversions nos. 1 (frame a), 3 (frame b), and 4 (frame c) (see Table 2 for details) of the relaxation spectrum of Fig. 1. The solid and dashed lines on each frame represent, respectively, the prior and starting models used in the inversions, while the dotted line is the *a posteriori,* or inverted, model. The three inversions are distinguished by the adopted starting model.

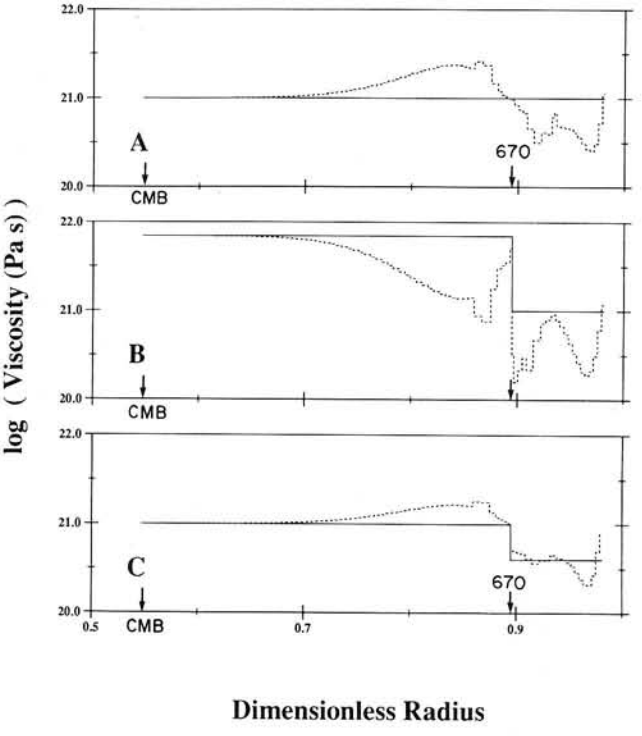

Figure 8. The results for inversion nos. 1 (frame a), 5 (frame b) and 6 (frame c) (see Table 2 for details) of the relaxation spectrum of Fig. 1. The solid line on each frame represents the prior and starting model use in the inversions, while the dotted line is the *a posteriori,* or inverted model. The three inversions are distinguished by the adopted *a priori* (and starting) model.

respective *a priori* models in the deep mantle reflecting the fact that the observational data provide no information regarding the rheology of this region. In the top half of the mantle, however, the *a posteriori* models are quite similar even though the *a priori* and starting models are fundamentally different. The only *apparent* discrepancy in this respect is evident in the *a posteriori* model of inversion no. 5 (Fig. 8b) which has a markedly stronger region at the top of the lower mantle and weaker transition zone than the inverted models 1 and 6. This raises a fundamentally important point. As discussed earlier, the relaxation spectrum data are not able to resolve structure in the transition zone independently of structure at the very top of the lower mantle (see Fig. 5). As a consequence, the *a posteriori* models may have very different values in these two regions. However, the *a posteriori* models must have consistent averages in the full region 1 (which extends from the top of the transition zone to 400 km within the lower mantle), since we have established that the rheology in that region is resolved by the relaxation spectrum data set. The summary statistics for inversions 1, 5 and 6 (Table 2) indicate that this is indeed the case.

Inversions nos. 1 through 6 have been performed using earth models with a 120 km lithosphere. McConnell (1968), Cathles (1975) and Wolf (1986) have recognized that an increase (decrease) in the lithospheric thickness used in their forward analyses could be compensated by an increase (decrease) in the viscosity of the sublithospheric region in order to fit the relaxation spectrum data set. In order to investigate this relationship we have, in inversions nos. 7, 8,

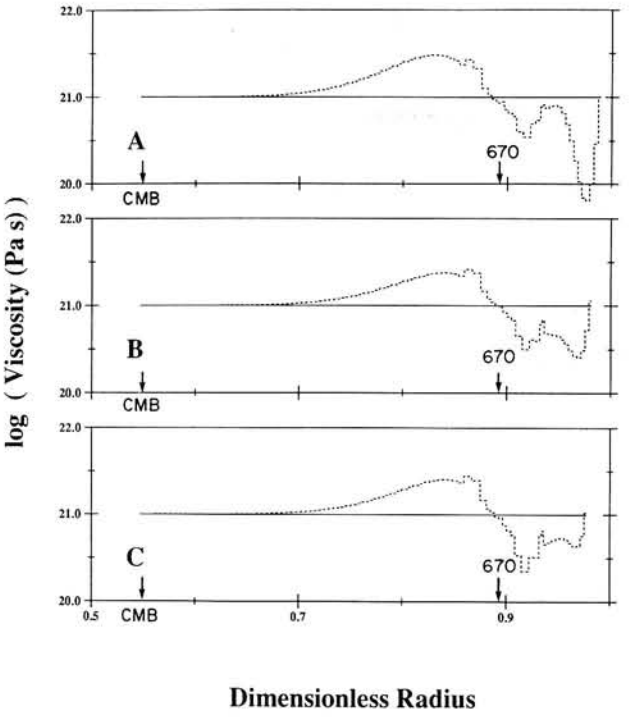

Figure 9. The results for inversion nos. 7 (frame a), 1 (frame b) and 9 (frame c) (see Table 2 for details) of the relaxation spectrum data set. The solid and dotted lines are defined on Fig. 8. The three inversions are distinguished by the value of the lithospheric thickness adopted in the calculations (70, 120 and 145 km, respectively).

and 9, considered Earth models with lithospheric thicknesses of 70, 100 and 145 km, respectively. The *a posteriori* models for inversions 7, 1 and 9 are shown on Figs 9(a), (b) and (c), respectively. Comparing the summary statistics for these inversions indicates that an increase in the lithospheric thickness leads to a small (and statistically relatively insignificant) decrease in the computed averages in the deepest regions 1 and 2. In contrast, in agreement with McConnell (1968) and Cathles (1975), the average logarithm of viscosity in region 3 (stretching from the base of the lithosphere to 235 km depth in all cases) is strongly dependent on the assumed lithospheric thickness. Indeed, the perturbation in the computed average increases almost linearly with the jump in the lithospheric thickness. Notice, for example, that the increase in the computed average between inversion nos. 8 and 9 (which have a 45 km difference in lithospheric thickness) is about 50 per cent larger than the increase between inversions nos. 7 and 8 (which have a 30 km difference in lithospheric thickness). The trend apparent on Table 2 confirms the assertion of Cathles (1975), who argued on the basis of forward calculations that the necessity of invoking a weak sublithospheric region (or low viscosity zone with respect to the underlying upper mantle) in order to fit the relaxation spectrum data disappears for sufficiently high lithospheric thicknesses (or, alternatively, flexural rigidities). In this respect the present results indicate that a lithospheric thickness greater than approximately 120 km would be required. Peltier (1984) has argued on the basis of relative sea-level data from the region peripheral to the Laurentide ice sheet that lithospheric thicknesses in excess of this may be required for shield areas (such as Fennoscandia).

Through a consideration of the intrinsic resolving power of the data the nine inversions discussed in this section have yielded robust constraints on the radial viscosity profile beneath Fennoscandia. In region 1, between 400 and 1040 km depth, the average logarithm of viscosity must be near 21.0 (or the logarithm of 10^{21} Pa s). In the overlapping region 2 extending from 210 km depth to the 670 km boundary between the upper and lower mantle the average is variable, but ranges between approximately 20.60 and 20.75 with an associated standard deviation of about 0.10. Finally, an average logarithm of viscosity significantly less than 21.0 is indicated in the sublithospheric region 3 for the class of Earth models with a lithospheric thickness less than 140 km.

The constraints summarized on Table 2 can be used to rule out a very large class of earth models. However, they also permit earth models with widely varying characteristics. In the discussion to follow we will introduce a set of such models in order to illustrate the non-uniqueness inherent to all inferences based on McConnell's (1968) Fennoscandian relaxation spectrum data and to emphasize that the only constraints that *all* models must satisfy are embodied in the summary statistics of Table 2.

The most direct approach to assessing the acceptability of a particular radial viscosity model is to compute the relaxation spectrum associated with the model and then consider whether that spectrum satisfies the observational constraint. Following eq. (6) we can define a statistic Q such that

$$Q(\mathbf{X}_G) = [\mathbf{y} - f(\mathbf{X}_G)]^T \mathbf{V}_\xi^{-1} [\mathbf{y} - f(\mathbf{X}_G)] \tag{11}$$

where $\mathbf{X}_G$ is an arbitrary viscosity model. Since the data vector $\mathbf{y}$ is assumed to have a Gaussian distribution, Q will be distributed as χ^2_n, where n is the number of spherical harmonic degrees included in the relaxation spectrum (in the case of Fig. 1, $n = 48$). Thus, a particular model $\mathbf{X}_G$ can be rejected at 99 per cent confidence if Q is greater than approximately 74. We will follow this procedure to assess the acceptability of the nine models summarized on Table 4.

Table 4 includes three sections: the first provides details of the radial layering used in the models and the logarithms of viscosity in each, as well as the lithospheric thickness (LT); the second lists the volumetric average of the logarithm of viscosity in the three regions specified on Table 3; and the third summarizes the results of the hypothesis test. While the viscosity of the models is specified down to the CMB, the details below about 1200 km depth (as described above) are relatively unimportant in terms of the computed misfit. The relaxation spectra computed on the basis of these nine models are shown on Figs 10, 11 and 12.

Let us consider the first model MC, which is adapted from the model preferred by McConnell (1968) in his analysis of the Fennoscandian relaxation spectrum. The model has a 120 km lithosphere and a relatively weak asthenosphere (extending to 400 km) overlying a uniform viscosity 10^{21} Pa s deep mantle (we have not included any of the viscosity increase below 800 km depth imposed by McConnell). Comparing this model to the *a posteriori* results from inversion no. 1 (which also used a 120 km lithosphere) indicates that it satisfies the constraints on the average value

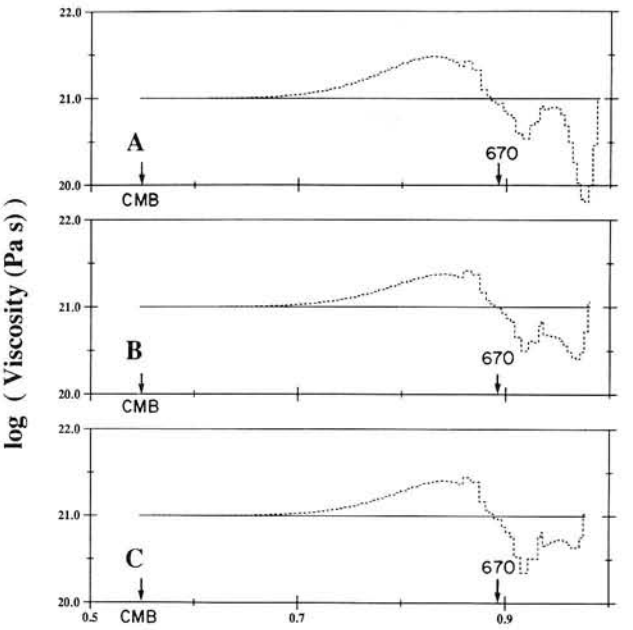

Figure 9. The results for inversion nos. 7 (frame a), 1 (frame b) and 9 (frame c) (see Table 2 for details) of the relaxation spectrum data set. The solid and dotted lines are defined on Fig. 8. The three inversions are distinguished by the value of the lithospheric thickness adopted in the calculations (70, 120 and 145 km, respectively).

and 9, considered Earth models with lithospheric thicknesses of 70, 100 and 145 km, respectively. The *a posteriori* models for inversions 7, 1 and 9 are shown on Figs 9(a), (b) and (c), respectively. Comparing the summary statistics for these inversions indicates that an increase in the lithospheric thickness leads to a small (and statistically relatively insignificant) decrease in the computed averages in the deepest regions 1 and 2. In contrast, in agreement with McConnell (1968) and Cathles (1975), the average logarithm of viscosity in region 3 (stretching from the base of the lithosphere to 235 km depth in all cases) is strongly dependent on the assumed lithospheric thickness. Indeed, the perturbation in the computed average increases almost linearly with the jump in the lithospheric thickness. Notice, for example, that the increase in the computed average between inversion nos. 8 and 9 (which have a 45 km difference in lithospheric thickness) is about 50 per cent larger than the increase between inversions nos. 7 and 8 (which have a 30 km difference in lithospheric thickness). The trend apparent on Table 2 confirms the assertion of Cathles (1975), who argued on the basis of forward calculations that the necessity of invoking a weak sublithospheric region (or low viscosity zone with respect to the underlying upper mantle) in order to fit the relaxation spectrum data disappears for sufficiently high lithospheric thicknesses (or, alternatively, flexural rigidities). In this respect the present results indicate that a lithospheric thickness greater than approximately 120 km would be required. Peltier (1984) has argued on the basis of relative sea-level data from the region peripheral to the Laurentide ice sheet that lithospheric thicknesses in excess of this may be required for shield areas (such as Fennoscandia).

Through a consideration of the intrinsic resolving power of the data the nine inversions discussed in this section have yielded robust constraints on the radial viscosity profile beneath Fennoscandia. In region 1, between 400 and 1040 km depth, the average logarithm of viscosity must be near 21.0 (or the logarithm of 10^{21} Pa s). In the overlapping region 2 extending from 210 km depth to the 670 km boundary between the upper and lower mantle the average is variable, but ranges between approximately 20.60 and 20.75 with an associated standard deviation of about 0.10. Finally, an average logarithm of viscosity significantly less than 21.0 is indicated in the sublithospheric region 3 for the class of Earth models with a lithospheric thickness less than 140 km.

The constraints summarized on Table 2 can be used to rule out a very large class of earth models. However, they also permit earth models with widely varying characteristics. In the discussion to follow we will introduce a set of such models in order to illustrate the non-uniqueness inherent to all inferences based on McConnell's (1968) Fennoscandian relaxation spectrum data and to emphasize that the only constraints that *all* models must satisfy are embodied in the summary statistics of Table 2.

The most direct approach to assessing the acceptability of a particular radial viscosity model is to compute the relaxation spectrum associated with the model and then consider whether that spectrum satisfies the observational constraint. Following eq. (6) we can define a statistic Q such that

$$Q(\mathbf{X}_G) = [\mathbf{y} - f(\mathbf{X}_G)]^T \mathbf{V}_\xi^{-1} [\mathbf{y} - f(\mathbf{X}_G)] \tag{11}$$

where $\mathbf{X}_G$ is an arbitrary viscosity model. Since the data vector $\mathbf{y}$ is assumed to have a Gaussian distribution, Q will be distributed as χ^2_n, where n is the number of spherical harmonic degrees included in the relaxation spectrum (in the case of Fig. 1, $n = 48$). Thus, a particular model $\mathbf{X}_G$ can be rejected at 99 per cent confidence if Q is greater than approximately 74. We will follow this procedure to assess the acceptability of the nine models summarized on Table 4.

Table 4 includes three sections: the first provides details of the radial layering used in the models and the logarithms of viscosity in each, as well as the lithospheric thickness (LT); the second lists the volumetric average of the logarithm of viscosity in the three regions specified on Table 3; and the third summarizes the results of the hypothesis test. While the viscosity of the models is specified down to the CMB, the details below about 1200 km depth (as described above) are relatively unimportant in terms of the computed misfit. The relaxation spectra computed on the basis of these nine models are shown on Figs 10, 11 and 12.

Let us consider the first model MC, which is adapted from the model preferred by McConnell (1968) in his analysis of the Fennoscandian relaxation spectrum. The model has a 120 km lithosphere and a relatively weak asthenosphere (extending to 400 km) overlying a uniform viscosity 10^{21} Pa s deep mantle (we have not included any of the viscosity increase below 800 km depth imposed by McConnell). Comparing this model to the *a posteriori* results from inversion no. 1 (which also used a 120 km lithosphere) indicates that it satisfies the constraints on the average value

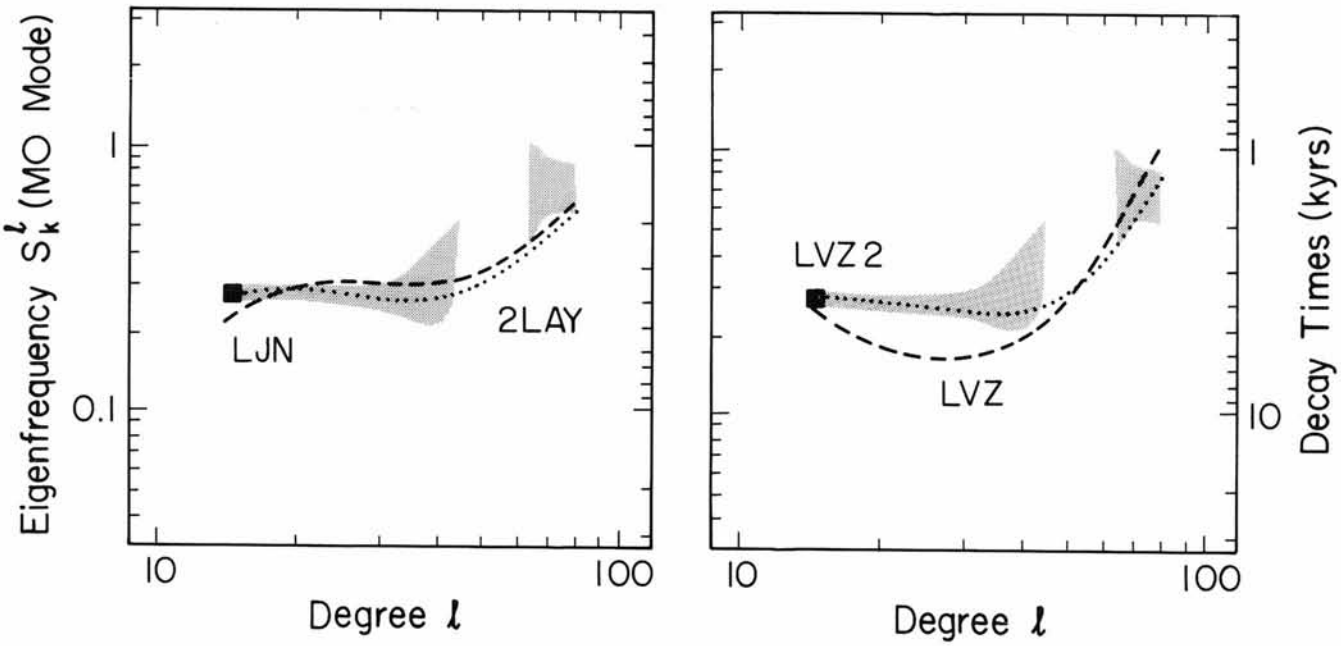

Figure 11. (See Fig. 1.) The lines labelled LJN, 2LAY, LVZ and LVZ2 refer to the relaxation spectra of the fundamental (MO) mode of decay computed using the associated rheological models summarized on Table 4.

of the *a posteriori* 'two layer' results on this parameter, we have performed analogous inversions (i.e. inversions performed assuming perfect correlations amongst model parameters in the upper and, separately, the lower mantle) for lithospheric thicknesses of 70, 120 and 145 km. The *a posteriori* model values in the upper and lower mantle for all four of these two layer versions (including LT = 100 km) are given on Table 5. The *a posteriori* standard deviations for the model values are all less than 0.001, indicating that if one were able to rigorously justify such a strong constraint on the model space, the *a posteriori* results would be exceedingly well determined.

The results on Table 5 indicate that the *a posteriori* model value in the upper mantle increases as the lithospheric thickness increases. Recall, in inversions which assumed no correlation amongst the model layers (Table 2) an increase in lithospheric thickness was associated with an increase in the viscosity at the top of the upper mantle in region 3 (in order that the model fit the short relaxation times which characterize the relaxation spectrum at high degrees).

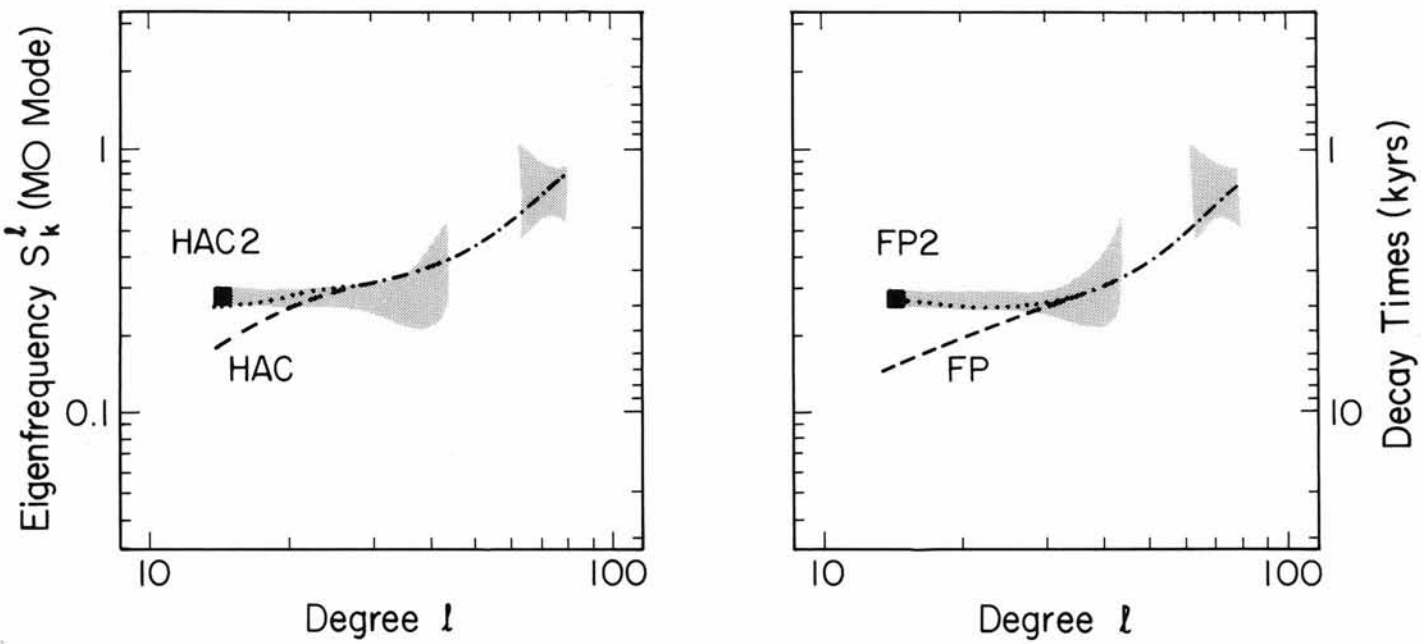

Figure 12. (See Fig. 1). The lines labelled HAC, HAC2, FP and FP2 refer to the relaxation spectra of the fundamental mode (MO) of decay computed using the associated rheological models summarized on Table 4.

Table 5. Results: two-layer (UM, LM) inversions.

LITHOSPHERIC THICKNESS (KM)	70	100	120	145
$<\text{LOG } \nu_{LM}>$	21.34	21.32	21.30	21.27
$<\text{LOG } \nu_{UM}>$	20.57	20.60	20.62	20.65

Limiting the model space to a single layer in the upper mantle tends to dampen this trend since the model must simultanesouly satisfy constraints on the average value in both regions 2 and 3. As a final point, the increase in the upper mantle model value, as the lithospheric thickness is increased, is matched by a decrease in the lower mantle model value on Table 5. This is necessary in order that the average value in region 1 (which extends across the 670 km boundary) remains near 21. As a consequence, the *a posteriori* results for a 'two-layer' viscosity model with a lithospheric thickness of 145 km, has a preferred viscosity jump of approximately 4 across the 670 km boundary.

Returning to Table 4, let us consider model LVZ, in which a region of weakness is constrained to occur in a very thin (90 km) low-viscosity zone (LVZ) overlaying a mantle of uniform viscosity. This type of model, in slightly altered forms, has been proposed by Cathles (1975) and Fjeldskaar & Cathles (1991) on the basis of their analysis of the glacial isostatic adjustment of Fennoscandia. In particular, Fjeldskaar & Cathles (1991) considered both the present day adjustment of the region and tilt data at selected geographic locations.

A comparison of the average value of model LVZ in the three regions specified on Table 3 (see Table 4) with the *a posteriori* results of inversion no. 7 on Table 2 indicates that the average value of the viscosity in region 2 is too stiff to fit the relaxation spectrum. This is verified on Fig. 11 where the relaxation spectrum computed using model LVZ exhibits decay times which are too long at intermediate degrees (which, as described earlier, are sensitive to the viscosity in region 2), and on Table 4 where the misfit statistic Q is unacceptably large.

Using the *a posteriori* constraints of inversion no. 7 as a guideline we have modified model LVZ to construct a model, which we denote as LVZ2, which includes a low viscosity zone and which fits the relaxation spectrum (see Fig. 11 and the statistic Q on Table 4). Model LVZ2 is characterized by a thin sublithospheric region with a viscosity one order of magnitude less than that of the underlying mantle. Furthermore, the model has constant viscosities in the upper mantle (below 160 km depth) and lower mantle of, respectively, 5×10^{20} Pa s and 1.5×10^{21} Pa s. The average value of model LVZ2, in the three regions specified on Table 4, differs most significantly from model LVZ in region 2. In contrast to model LVZ, the average value for model LVZ2 in that region (20.7) matches the *a posteriori* constraint generated from inversion no. 7, and this leads to the excellent fit evident on Fig. 11.

A comparison of models LVZ2 and 2LAY raises an interesting point. In model LVZ2 the upper mantle is discretized into two layers of constant viscosity. The *a posteriori* constraints on the average value of the model in regions 1 and 2 (see inversion no. 7 on Table 2) can therefore be satisfied by varying the viscosity in both these regions. As a consequence, the requirement for a weak sublithospheric region impacts much less on the viscosity below 160 km depth in model LVZ2 than it does on model 2LAY which limits the model space to a single layer in the upper mantle. The result, evident on Table 4, is that model LVZ2 is permitted a stiffer region below 160 km depth, and a weaker region below 670 km depth in order to satisfy the *a posteriori* constraint on the average model value in region 1, leading to a very moderate factor of three jump in viscosity across 670 km depth.

To conclude this section consider the models HAC and FP on Table 4, both of which were derived from analyses of the earth's long wavelength geoid and plate motions driven by the convective circulation in the planetary interior. As an example, Forte, Peltier & Dziewonski (1991) considered a formal five-layer inversion of the data sets and found that the model FP satisfied the *a posteriori* statistics of their analysis. In a forward analysis of the data sets, Hager (1991) preferred a model similar to HAC, except with an asthenospheric viscosity of 2.5×10^{19} Pa s (or 19.43 in logarithm space; let us call this model HA). Hager (1991) has, however, argued that the model HA may not be characteristic of regions below continental environments, and has suggested that an increase of the asthenospheric viscosity of less than or equal to a factor of 10 would be required to fit uplift data over regions such as Fennoscandia. Accordingly, model HAC is constructed to have an order of magnitude larger viscosity in the asthenosphere (2.5×10^{20} Pa s) than model HA.

Table 4 indicates that both model HAC and FP have average values in region 1 which are substantially stiffer than are allowed by the *a posteriori* constraints provided by inversion no. 8 on Table 2. Not surprisingly, both models have misfit statistics Q which are unacceptably large. This misfit is also apparent on Fig. 12 which shows the relaxation spectra computed using the two models (note the large misfits at the longest wavelengths).

The source of the misfit is clearly the rather stiff lower mantle viscosities which characterize both models HAC and FP. Accordingly, we have constructed two alternate models, HAC2 and FP2, by simply reducing the lower mantle viscosities in, respectively, models HAC and FP, until the *a posteriori* constraint on the average model value in region 1 was satisfied. In the case of model HAC2, the lower mantle viscosity has been reduced to approximately 2×10^{21} Pa s (from 6×10^{21} Pa s), while in the case of model FP2 the reduction is to 10^{21} Pa s (from 4.2×10^{21} Pa s). Neither model HAC2 or FP2 can be rejected at 99 per cent confidence on the basis of the misfit statistic Q, although model HAC2 represents a borderline model in this respect. [Note, from Fig. 12, that model HAC2 produces decay times for degrees near 30 which are slightly too short compared to the observational constraint; this indicates that the average value of the model in region 2 (20.63), which these intermediate degrees are most sensitive to, is slightly too weak. This can be corrected by increasing the asthenospheric viscosity of the 'continental' model HAC (and HAC2) by slightly more than a factor of 10 over the value of model HA.]

The result of our modifications (HAC2, FP2) is to produce models with markedly smaller viscosity contrasts

from the base of the lithosphere to the deep mantle. Notice, in this respect, that the modifications have yielded models which are somewhat similar to McConnell's (1968) model MC on Table 4. As a final point, we emphasize that the modifications to models HAC and FP are only required at the top of the lower mantle (above approximately 1200 km depth) and the viscosity profiles of these models below this depth will be of little consequence to their fit to the Fennoscandian relaxation spectrum.

4 CONCLUSIONS

The large data base of geophysical observables which reflect the glacial isostatic adjustment process serves as a primary source for inferences of mantle rheology. In this paper we have examined a now-classic subset of this data base; the relaxation spectrum of Fennoscandia originally derived by McConnell (1968) from his analysis of the uplift pattern of that region. In this regard, we have used a Monte Carlo approach, with conservative random-error perturbations, to rederive the spectrum together with its associated uncertainties and cross-correlations. Our inversions of the data base, formulated using the theory of non-linear Bayesian inference, have yielded a set of robust constraints which *all* models for the radial viscosity variation below Fennoscandia must satisfy (Table 2). The constraints are consistent with the resolving power of the relaxation spectrum data set and incorporate estimates of uncertainty.

The relaxation spectrum discussed in this study represents the set of eigenfrequencies for the fundamental modes of viscous gravitational relaxation between spherical harmonic degrees 14 and 45 as well as 65 to 80. Theoretical predictions of the spectrum are based on the solution of the homogeneous problem (Peltier 1976) and therefore the constraints provided by the observational data set are, in theory, independent of the surface loading history (that is, independent of the excitation of the normal modes), and therefore any uncertainties associated with that history. We have used these constraints to construct a set of models which illustrate the non-uniqueness inherent to the acceptable model solution space. The constraints have also been applied, together with a statistic (eq. 11) based upon the computed misfit to the 'observed' relaxation spectrum, to rule out a number of published viscosity models.

An assumption of isoviscous upper and lower mantle regions is common in inferences of mantle viscosity based upon the glacial isostatic adjustment data set. As an example, on the basis of their forward analysis of sea-level variations in northwestern Europe, Lambeck, Johnston & Nakada (1990) have proposed a model (LJN—Table 4) with a lithospheric thickness of 100 km and upper and lower mantle viscosities of, respectively, 3.5×10^{20} Pa s and 4.7×10^{21} Pa s. We have found that the model does not satisfy the relaxation spectrum data set (nor does it satisfy the *a posteriori* statistics generated from the inversion of that spectrum). We have, furthermore, performed inversions which assume perfect correlation amongst the model parameters in the upper, and, separately, the lower mantle, and those inversions suggest upper mantle viscosities in the range 3.7×10^{20}–4.5×10^{20} Pa s and lower mantle viscosities in the range 2.2×10^{21} Pa s–1.9×10^{21} Pa s. The ranges arise from the variation in the assumed lithospheric thickness, with the first number in each range associated with LT = 70 km and the second with LT = 145 km. In the context of two-layer models, the misfit computed for model LJN arises, primarily, from the overly stiff lower mantle of the model. If one were justified in assuming isoviscous upper and lower mantle regions, our two-layer inversions suggest a viscosity contrast across the 670 km boundary of between four and six (for the range of lithospheric thicknesses considered on Table 5).

The *a posteriori* constraints arising from the inversion of the relaxation spectrum also rule out a rheological profile consisting of a thin low-viscosity zone overlying a constant viscosity (10^{21} Pa s) deep mantle (model LVZ on Table 4). Such a model, in slightly altered form, has been proposed by Cathles (1975) and Fjeldskaar & Cathles (1991) on the basis of their analysis of the glacial isostatic adjustment of Fennoscandia. Nevertheless, we have constructed a similar model (LVZ2 on Table 4), consisting of a low-viscosity zone overlying a deep mantle characterized by a moderate (factor of 3) viscosity increase across 670 km depth, which fits the relaxation spectrum.

We have also used the Fennoscandian relaxation spectrum to test the acceptability of various viscosity models derived on the basis of long-wavelength geoid and plate-motion observations associated with the mantle convective circulation (Forte *et al.* 1991; Hager 1991). The model FP (Table 4), which was found by Forte *et al.* (1991) to be acceptable in terms of the *a posteriori* constraints from a five-layer inversion of the data sets, as well as model HAC (Table 4), which Hager (1991) has proposed as characteristic of regions below continental environments, have both been found to provide unsatisfactory fits to the relaxation spectrum. In this regard, our *a posteriori* constraints derived from the inversion of the relaxation spectrum, indicate that the source of the misfit is an overly stiff rheology in the shallowest part of the lower mantle (above about 1200 km depth) which characterizes these models. We have shown that modifications to the models, based on the reduction of viscosity in this part of the lower mantle, can produce models which fit the relaxation spectrum data set.

The non-uniqueness associated with the *a posteriori* constraints is evident in the number of models discussed herein which fit the Fennoscandian relaxation spectrum rederived in this paper. We have shown, for example, that a model (MC on Table 4) with a weak asthenosphere (down to 400 km depth) overlying an isoviscous 10^{21} Pa s deeper mantle provides an excellent fit to the spectrum. This fit is also possible (as discussed above) using models with a factor of roughly five jump in viscosity across the 670 km boundary between isoviscous upper and lower mantle regions (with the latter having a viscosity near 2×10^{21} Pa s), and models with a low viscosity zone overlying a two-layer deep mantle with a moderate (factor of three) viscosity contrast across 670 km depth.

Given the many uncertainties and complications associated with the derivation of the Fennoscancian relaxation spectrum (see McConnell 1968) a significant reduction in the associated observational uncertainty is difficult if not impossible. The non-uniqueness associated with the inferences described in this study can, however, be reduced by considering other obervational constraints associated with the region. In particular, in a companion paper

(Mitrovica & Peltier 1993) we use the *a posteriori* constraints derived in this study as the *a priori* constraints in an inversion of the observed RSL variations at the centre, edge and periphery of the ancient Fennoscandian ice complex.

ACKNOWLEDGMENTS

The work reported in this paper was supported in part by a grant to W.R.P. from the Climate and Global Change Program of the US National Oceanic and Atmospheric Administration (NOAA) in the area of Global Sea Level. It is part of a project to develop an ultra-high-resolution model of the postglacial rebound process for use in the 'decontamination' of tide gauge data. The research of J.X.M. at Harvard-Smithsonian has been supported in part by NSERC, the Smithsonian Institution and NASA Grant no. NAG5-1930. We thank J. L. Davis and A. M. Forte for their many constructive comments related to this research.

5 REFERENCES

Backus, G. E., 1971. Inference from inadequate and inaccurate data, *Lect. appl. Math.*, **14,** 1–105.

Backus, G. E., 1988. Bayesian inference in geomagnetism, *Geophys. J.R. astr. Soc.*, **92,** 125–142.

Backus, G. E. & Gilbert, J. F., 1968. The resolving power of gross Earth data, *Geophys. J.R. astr. Soc.*, **16,** 169–205.

Cathles, L. M., 1971. The viscosity of the Earth's mantle, *PhD thesis,* Princeton University, NJ.

Cathles, L. M., 1975. *The Viscosity of the Earth's Mantle,* Princeton University Press, Princeton, NJ.

Daly, R. A., 1934. *The Changing World of the Ice Age,* Yale University Press, New Haven, CT.

Ekman, M., 1991. A concise history of postglacial land uplift research (from its beginning to 1950), *Terra Nova,* **3,** 358–365.

Fjeldskaar, W. & Cathles, L. M. 1991. Rheology of mantle and lithosphere inferred from post-glacial uplift in Fennoscandia, in *Glacial Isostasy, Sea-Level and Mantle Rheology,* pp. 1–20, eds Sabadini, R., Lambeck, K. & Boschi, E., Proceedings of the NATO Advanced Research Workshop on Glacial Isostasy, Sea-Level and Mantle Rheology, NATO ASI Series V.334, Kluwer, The Netherlands.

Forte, A. M., Peltier, W. R. & Dziewonski, A. M., 1991. Inferences of mantle viscosity from tectonic plate velocities, *Geophys. Res. Lett.,* **18,** 1747–1750.

Goldreich, P. & Toomre, A., 1969. Some remarks on polar wandering, *J. geophys. Res.,* **74,** 2555–2567.

Gutenberg, B., 1941. Changes in sea level, postglacial uplift, and mobility of the Earth's interior, *Bull. geol. Soc. Am.,* **52,** 721–722.

Hager, B. H., 1991. Mantle viscosity: a comparison of models from postglacial rebound and from the geoid, plate deriving forces, and advected heat flux, in *Glacial Isostasy, Sea-Level and Mantle Rheology,* pp. 493–514, eds Sabadini, R., Lambeck, K. & Boschi, E., Proceedings of the NATO Advanced Research Workshop on Glacial Isostasy, Sea-Level and Mantle Rheology, NATO ASI Series V. 334, Kluwer, The Netherlands.

Haskell, N. A., 1935. The motion of a viscous fluid under a surface load. 1, *Physics,* **6,** 265–269.

Haskell, N. A., 1936. The motion of a viscous fluid under a surface load. 2, *Physics,* **7,** 56–61.

Jackson, D. D., 1979. The use of *a priori* data to resolve non-uniqueness in linear inversion, *Geophys. J.R. astr. Soc.,* **57,** 137–158.

Jackson, D. D. & Matsu'ura, M., 1985. A Bayesian approach to non-linear inversion, *J. geophys. Res.,* **90,** 581–591.

Lambeck, K., Johnston, P. & Nakada, M., 1990. Holocene glacial rebound and sea-level change in NW Europe, *Geophys. J. Int.,* **103,** 451–468.

McConnell, R. K., 1968. Viscosity of the mantle from relaxation time spectra of isostatic adjustment, *J. geophys. Res.,* **73,** 7089–7105.

Mitrovica, J. X. & Peltier, W. R., 1991. A complete formalism for the inversion of post-glacial rebound data: resolving power analysis, *Geophys. J. Int.,* **104,** 267–288.

Mitrovica, J. X. & Peltier, W. R., 1993. The inference of mantle viscosity from the inversion of relative sea level variations in Fennoscandia, *in preparation.*

Munk, W. H. & MacDonald, G. J. F., 1960. *The Rotation of the Earth,* Cambridge University Press, London.

Niskannen, E., 1939. On the upheaval of land in Fennoscandia, *Ann. Acad. sci. Fennicae.,* **53,** 1–30.

Parsons, B. D., 1972. Changes in the Earth's shape, *PhD thesis,* Cambridge University.

Peltier, W. R., 1974. The impulse response of a Maxwell Earth, *Rev. Geophys. Space Phys.,* **12,** 649–669.

Peltier, W. R., 1976. Glacial isostatic adjustment II. The inverse problem, *Geophys. J.R. astr. Soc.,* **46,** 669–706.

Peltier, W. R., 1982. Dynamics of the ice age Earth, *Adv. Geophys,* **24,** 1–146.

Peltier, W. R., 1984. The thickness of the continental lithosphere. *J. geophys. Res.,* **89,** 11303–11316.

Peltier, W. R., 1985. The LAGEOS constraint on deep mantle viscosity: results from a new normal model method for the inversion of visco-elastic relaxation spectra, *J. geophys. Res.,* **90,** 9411–9421.

Sauramo, M. R., 1958. Die geschichte der Ostsee, *Ann. Acad. Sci. Fennicae,* A.

Tarantola, A. & Valette, B., 1982a. Inverse problems = quest for information, *J. Geophys.,* **50,** 159–170.

Tarantola, A. & Valette, B., 1982b. Generalized non-linear inverse problems solved using the least squares criterion, *Rev. Geophys. Space Phys.,* **20,** 219–232.

Tushingham, A. M., 1989. A global model of late Pleistocene deglaciation: implications for Earth structure and sea level change, *PhD thesis,* University of Toronto, Toronto, Canada.

Van Bemmelen, R. W. & Berlage, H. P., 1935. Versuch einer Mathematischen Behandlung Geotektonischer Bewegungen unter besonderer Berücksichtiging der Undationstheorie, *Gerlands Beitr. Geophys.,* **43,** 19–55.

Vening-Meinesz, F. A., 1937. The determination of the Earth's plasticity from the postglacial uplift of Scandinavia: isostatic adjustment, *Koninklijke Akademie van Weter-Schapper,* **40,** 654–662.

Walcott, R. J., 1972. Late Quaternary vertical movements in eastern North America, *Rev. Geophys. Space Physics,* **10,** 849–884.

Wolf, D., 1986. Glacio-isostatic adjustment in Fennoscandia revisited, *J. Geophys.,* **59,** 42–48.

Wu, P. & Peltier, W. R., 1982. Viscous gravitational relaxation, *Geophys. J.R. astr. Soc.,* **70,** 435–486.